FABRICATION OF POLYMETHYL METHACRYLATE STRUCTURE BY 3DP FOR MEDICAL APPLICATIONS

PANTIDA PATIRUPANUSARA

A THESIS SUBMITTED IN PARTIAL FULFILLMENT
OF THE REQUIREMENTS FOR
THE DEGREE OF MASTER OF ENGINEERING
(BIOMEDICAL ENGINEERING)
FACULTY OF GRADUATE STUDIES
MAHIDOL UNIVERSITY
2006

ISBN 974-04-7762-3

Thesis
Entitled

FABRICATION OF POLYMETHYL METHACRYLATE STRUCTURE BY 3DP FOR MEDICAL APPLICATIONS

Pantida Patirupanusara..
Miss Pantida Patirupanusara
Candidate

Jintamai Suwaprateeb
Mr. Jintamai Suwanprateeb,
Ph.D. (Biomaterials)
Major-Advisor

Theeraporn Rubcumintara
Assist.Prof. Theeraporn Rubcumintara,
Ph.D. (Materials Engineering & Science)
Co-Advisor

Prof. M.R. Jisnuson Svasti, Ph.D.
Dean
Faculty of Graduate Studies

Theeraporn Rubcumintara
Assist.Prof. Theeraporn Rubcumintara,
Ph.D. (Materials Engineering & Science)
Chair
Master of Engineering Programme in
Biomedical Engineering
Faculty of Engineering

Thesis
Entitled

FABRICATION OF POLYMETHYL METHACRYLATE STRUCTURE BY 3DP FOR MEDICAL APPLICATIONS

was submitted to the Faculty of Graduate Studies, Mahidol University
for the degree of Master of Engineering (Biomedical Engineering)
on
5 October, 2006

Pantida Patirupanusara.
Miss Pantida Patirupanusara
Candidate

Assist.Prof. Jackrit Suthakorn,
Ph.D. (Mechanical Engineering)
Chair

Jintamai Suwanprateeb
Mr. Jintamai Suwanprateeb,
Ph.D. (Biomaterials)
Member

Theeraporn Rubcumintara
Assist.Prof. Theeraporn Rubcumintara,
Ph.D. (Materials Engineering & Science)
Member

Khemchai Hemachandra
Assoc.Prof. Khemchai Hemachandra,
Ph.D. (Biomaterials)
Member

Prof. M.R. Jisnuson Svasti, Ph.D.
Dean
Faculty of Graduate Studies
Mahidol University

Assist.Prof. Piya Rattanasuwan,
M.Eng.
Dean
Faculty of Engineering
Mahidol University

ACKNOWLEDGEMENT

I would like to express my gratitude to all who gave me the possibility to complete this thesis. First of all, I would like to express my appreciation to my thesis advisor, Dr.Jintamai Suwanprateeb, for giving me the opportunity to participate in this work, his valuable suggestions and his support throughout my time at MTEC. I am sincerely grateful to Assist.Prof.Dr. Theeraporn Rubcumintara, a member of my advisory committee, for valuable suggestions and constructive comments for editing this thesis. Assoc.Prof.Dr. Khemchai Hemachandra from Chulalongkorn University is thanked for his insightful comments and participating in the defense. Dr.Jackrit Suthakorn is thanked for his comment and advice.

I am grateful to the National Metal and Materials Technology Center (MTEC) for all the support in enabling me to undertake this research. My gratitude also to Dr.Kriskrai Sitthiseripratip, Mr.Natapoom Vatanapatimakul and all the shared knowledge from Computer Aided Medical Technology Laboratory for their care and precious friendship during my stay at MTEC. I also want to thank Miss Waraporn Suwanpreuk for her friendship and technical support. Miss Somreuthai Channasanont is thanked for the supply of acrylic sealant.

I would like to thank all my friends at the Biomedical Engineering Programme for their interest, encouragement and support during the course of my work. I am also grateful for the assistance I received from many undergraduate and graduate students in the Biomedical Engineering Programme, especially Pracha Yambangyang for the inspiring discussions and materials support.

Finally, I would like to thank my parents for their unlimited love, their understanding, financial and emotional support throughout my studies and my life.

Pantida Patirupanusara

FABRICATION OF POLYMETHYL METHACRYLATE STRUCTURE BY 3DP FOR MEDICAL APPLICATIONS

PANTIDA PATIRUPANUSARA 4536772 EGBE/M

M.Eng.(BIOMEDICAL ENGINEERING)

THESIS ADVISORS: JINTAMAI SUWANPRATEEB, Ph.D.(BIOMATERIALS), THEERAPORN RUBCUMINTARA, Ph.D. (MATERIALS ENGINEERING AND SCIENCE)

ABSTRACT

Three dimensional printing (3DP) is one rapid prototyping technique, which creates parts directly from graphical data in computers. Since the 3DP process cannot fabricate biomaterials directly, the 3DP model is normally printed and employed as a pattern of the desired implants to create moulds for further casting by biomaterials. This research was carried out to formulate polymethyl methacrylate (PMMA) based mixture suitable to be directly fabricated in the 3DP machine and to determine the influence of mixture composition and post-processing technique on the physical and mechanical properties of the structures. This involved initially making a green structure by printing a binder onto the different formulations of mixture of PMMA and water soluble adhesive powder. The results show that PMMA structures were directly fabricated by 3DP. Variation of the percentage of mixture composition affects the formability and structural quality of as-fabricated samples including dimension accuracy, porosity, bulk density and flexural and compressive properties. Infiltration by heat-cured acrylic resin enhances modulus, strength of structures to be close to conventional indirect fabricated PMMA resin. It was observed that the optimum formulation was determined to be 80% PMMA, 10% maltodextrin and 10% PVA. The properties of the directly fabricated PMMA parts from this investigation are sufficient as an alternative to PMMA parts made by the conventional indirect fabrication method. These structures can be developed as cranio-maxillofacial implants, dental implants and a variety of other biomedical applications.

KEY WORDS: MEDICAL/ RAPID PROTOTYPING/ THREE DIMENSIONAL PRINTING/ 3DP/ 3D-PRINTING/ PMMA

79 P. ISBN 974-04-7762-3

การขึ้นรูปชิ้นงานพอลิเมทิลเมทาคริเลทโดยเทคโนโลยีการพิมพ์ 3 มิติ สำหรับการใช้งานทางการแพทย์ (FABRICATION OF POLYMETHYL METHACRYLATE STRUCTURE BY 3DP FOR MEDICAL APPLICATIONS)

พรรธิดา ปฏิรูปานุสร 4536772 EGBE/M

วศ.ม. (วิศวกรรมชีวการแพทย์)

คณะกรรมการควบคุมวิทยานิพนธ์ : จินตมัย สุวรรณประทีป, Ph.D. (Biomaterials), ธีรพร รับคำอินทร์, Ph.D. (Materials Engineering and Science)

บทคัดย่อ

เครื่องพิมพ์สามมิติเป็นหนึ่งในเทคโนโลยีสร้างต้นแบบรวดเร็วที่สามารถสร้างแบบจำลองสามมิติได้จากภาพสามมิติในคอมพิวเตอร์ อย่างไรก็ตาม วัตถุดิบทางการค้าสำหรับเครื่องพิมพ์สามมิตินี้โดยทั่วไปไม่สามารถใช้เป็นวัสดุฝังในจากวัสดุทางการแพทย์ได้โดยตรง แบบจำลองสามมิติที่สร้างขึ้นจากเครื่องพิมพ์สามมิติได้ถูกนำมาใช้ทำแม่แบบเพื่อเป็นแบบสำหรับการหล่อวัสดุฝังในด้วยวัสดุทางการแพทย์ งานวิจัยชิ้นนี้ศึกษาการพัฒนาส่วนผสมของพอลิเมอร์ที่เหมาะสำหรับการขึ้นรูปชิ้นงานพอลิเมทิลเมทาคริเลทโดยเทคโนโลยีการพิมพ์ 3 มิติ และทำการศึกษาถึงผลกระทบของส่วนผสมต่างๆ ได้แก่ พอลิเมทิลเมทาคริเลท มัลโตเด็กซ์ทริน และพอลิไวนิล แอลกอฮอล์ วิธีการเริ่มจากการขึ้นรูปชิ้นงานโดยการพ่นของเหลวที่มีส่วนประกอบของน้ำจากเครื่องพิมพ์สามมิติ ลงบนส่วนผสมต่างๆของผงพอลิเมทิลเมทาคริเลท กับผงมัลโตเด็กซ์ทริน และ พอลิไวนิลแอลกอฮอล์ที่ละลายน้ำได้และทำหน้าที่เป็นกาวยึดส่วนผสมเข้าด้วยกัน จากการศึกษาพบว่าสามารถขึ้นรูปชิ้นงานพอลิเมทิลเมทาคริเลทได้โดยตรงโดยเครื่องพิมพ์ 3 มิติ การเปลี่ยนแปลงอัตราส่วนผสมข้างต้น ส่งผลต่อสมบัติของชิ้นงานที่ขึ้นรูป ได้แก่ ความถูกต้องของขนาด จำนวนรูพรุน ความหนาแน่นของชิ้นงาน ตลอดจนสมบัติทางเชิงกล เช่น ค่ามอดูลัสและความต้านทางแรงสูงสุดของชิ้นงาน นอกจากนี้การอัดแทรกชิ้นงานด้วยอะคริลิคเรซิน สามารถเพิ่มค่ามอดูลัส และความต้านทานแรงสูงสุดของชิ้นงานของทั้งการดัดงอและการบีบอัดให้มีค่ามากขึ้นใกล้เคียงกับเรซินอะคริลิคที่ใช้งานทางการแพทย์ ซึ่งพบว่าสัดส่วนที่เหมาะสมประกอบไปด้วย พอลิเมทิลเมทาคริเลท ร้อยละ 80 มัลโตเด็กซ์ทริน ร้อยละ 10และ พอลิไวนิลแอลกอฮอล์ ร้อยละ 10 เมื่อนำมาเปรียบเทียบกับชิ้นงานพอลิเมทิลเมทาคริเลทที่ได้จากการหล่อโดยเรซินอะคริลิคที่ใช้งานทางการแพทย์ทั่วไป พบว่า ชิ้นงานพอลิเมทิลเมทาคริเลทที่ได้ สามารถทดแทนชิ้นงานที่ได้จากการหล่อด้วยเรซินอะคริลิคทางการค้าที่ใช้อยู่ในปัจจุบันได้ ชิ้นงานพอลิเมทิลเมทาคริเลทที่ขึ้นรูปโดยตรงจากเครื่องพิมพ์สามมิตินี้ สามารถพัฒนาเพื่อผลิตวัสดุฝังในที่มีรูปร่างซับซ้อน เช่น วัสดุฝังในที่ใช้ในการผ่าตัดแก้ไขความบกพร่องบริเวณกระโหลกศีรษะ ใบหน้า และขากรรไกร ตลอดจนงานทันตกรรม รวมไปถึงงานด้านชีวการแพทย์อื่นๆอีกด้วย

79 หน้า ISBN 974-04-7762-3

CONTENTS

CONTENTS (continued)

CONTENTS (continued)

LIST OF TABLES

LIST OF FIGURES

LIST OF FIGURES (Continued)

LIST OF FIGURES (Continued)

LIST OF EQUATIONS

CHAPTER I
INTRODUCTION

1.1 Background

Nowadays, rapid prototyping (RP) has been utilized in biomedical applications ranging from a pre- or per-operative planning model for surgeons [1-2] to the design and building of medical implants and devices [3-4]. Rapid prototyping is a process that fabricates solid objects from 3D computer data by relatively new additive technologies [5]. Three dimensional printing (3DP) is one of commercially available RP machines that involves the selectively joining of powdered materials with binder from an inkjet print head layer by layer. This technique allows the complex physical structures to be fabricated rapidly and accurately using 3D computer data.

In maxillofacial and craniofacial application, cranio-maxillofacial defects resulting from cranial bone tumours, traumatic injury, external decompression and infectious lesions are often severe enough to warrant surgical reconstruction [4,6]. These bone defects require treatment for medical and cosmetic reasons. Many techniques have been used for the closure of the cranio- maxillofacial defects. A widely used method is implanting polymethyl methacrylate (PMMA) cement which is manually shaped and cured in the operating room by surgeon [4]. This process is time-consuming and prone to cosmetic compromise. Due to the advances in bioengineering, customized templates and implants are now available for maxillofacial and craniofacial reconstruction using rapid prototyping technology. Rapid prototyping makes it possible to design and fabricate a customized implant that precisely fits individual patient prior to the surgery. However, biomedical implants that are usually made from polymethyl methacrylate can not be directly fabricated by 3DP machine. In order to fabricate the biomedical implants, the 3DP model is fabricated and employed as a pattern of the desired implants to create silicone or plaster moulds for further casting by polymethyl methacrylate.

This research is aimed to formulate the suitable polymethyl methacrylate based powder for three dimensional printing machine focusing on the cranio-maxillofacial reconstruction.

1.2 Problem Statement

The materials supplied with the three dimensional printing machine (starch-based powder and plaster-based powder) are generally designed for industrial works and can not be directly implanted in the body. Therefore, the use of these materials to fabricate medical implants is not recommended. The conventional indirect fabrication method uses the 3DP model to generate a plaster mold for the conversion of 3DP model into implant. This method involves many processing steps and long manufacturing time. These cause extra costs of the implants.

1.3 Goals of the Thesis

Objectives of this research study are demonstrated as following:

1. To formulate polymethyl methacrylate based powder suitable to be fabricated by 3DP machine.

2. To determine the influence of mixture composition and post-processing technique on physical and mechanical properties of the structures.

1.4 Expected Result

Polymethyl methacrylate (PMMA) can be used to directly fabricate specimen using available three dimensional printing machine. The properties of the directly fabricated PMMA parts from this investigation are expected to be sufficient as an alternative to the PMMA parts made from conventional indirect fabrication method. Direct fabrication of PMMA parts will result in minimizing complicated procedures, reducing manufacturing time and saving costs.

CHAPTER II
LITERTURE REVIEW

In this chapter, a brief introduction to rapid prototyping technology, medical applications of rapid prototyping, medical rapid prototyping process and the commercial polymethyl methacrylate for biomedical applications are presented. The last part of this paper gives the information about the biocompatibility and the properties of the materials, which were involved in this study.

2.1 Rapid prototyping technology

2.1.1 What is rapid prototyping?

Rapid prototyping (RP) is a technique that can fabricate complex-shaped, three-dimensional parts directly from graphical data in computer. Raw image data can be acquired either from a CAD software, computed tomography (CT) scan or magnetic resonance imaging (MRI). The system is also known by the other names as freeform fabrication (FFF), solid freeform fabrication (SFF) and layered manufacturing [7].

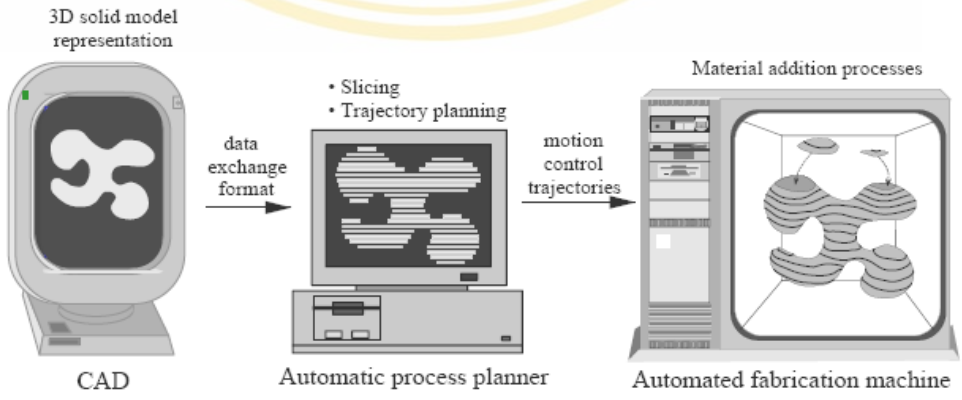

Figure 2.1 Solid freeform fabrication using layered manufacturing paradigm [8]

Rapid prototyping machines process graphical data by slicing the model into thin layers using a software package. Each layer is typically about 0.1-0.25 mm in thickness. The machine then uses these sliced data to construct the solid model layer by layer additively until the desired shape is achieved [9]. This is in contrast to traditional machining processes, such as milling, drilling, and grinding which are subtractive processes that remove materials from a solid block. This allows rapid prototyping technique to create objects with complicated internal features that cannot be manufactured by other means in a short duration.

2.1.2 Benefits and Limitations of RP

The prototypes created from RP have numerous uses. They make excellent visual aids for communicating proposes. In addition, prototypes can be used for design testing. For example, an aerospace engineer might mount a model airfoil in a wind tunnel to measure lift and drag forces [10]. For small production runs and complicated objects, rapid prototyping is often the optimal process available. Most prototypes require three to seventy-two hours to build, depending on the size and complexity of the object. It is much faster than the weeks or months required to make prototypes by traditional methods. Using RP technology typically reduces the time and cost of producing prototypes by 30-90% [11]. Another advantage is that excess material is not wasted [12]. However, the materials used in rapid prototyping are limited and dependent on the method chosen. These include plastics, ceramics, metals ranging from stainless steel to titanium and wood-like paper [7].

2.1.3 The Basic Process

There are several rapid prototyping techniques, but all work under the same basic process [10]. The steps are shown in figure 2.2.

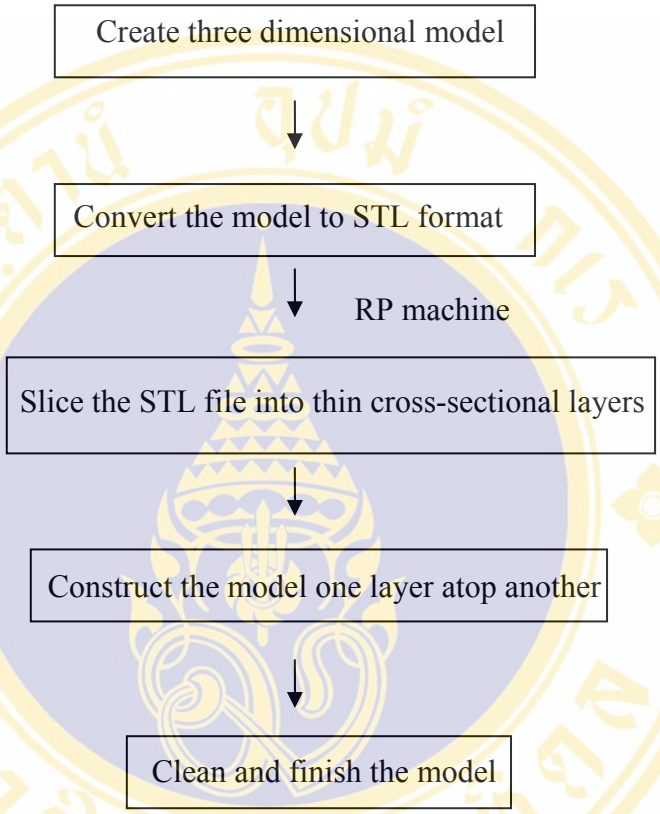

Figure 2.2 Diagram of basic rapid prototyping process [10]

2.1.4 Overview of Some RP Processes

At least five different rapid prototyping techniques are commercially available [5,10]. Each has unique strengths and weaknesses. These are stereolithography (SLA), selective laser sintering (SLS), fused deposition modeling (FDM), laminated object manufacturing (LOM) and three dimensional printing (3DP).

2.1.4.1 Stereolithography (SLA)

Stereolithography is the pioneer of the rapid prototyping industry in which the first commercial system introduced in 1988 by 3D Systems, Inc.[13]. It builds plastic parts layer-by-layer using laser-scanning of light sensitive photopolymer in the area defined by the object's cross-section. The photopolymer is solidified by the laser light [7]. Once one layer is completely traced, it is lowered one layer into the liquid and a subsequent layer is traced and adhered to the previous layer. After many such layers are traced, a complete 3D model is formed. The model is then placed in an ultraviolet oven to harden uncured resin. Stereolithography generally is considered to provide the greatest accuracy and best surface finish of any rapid prototyping technologies [7,13].

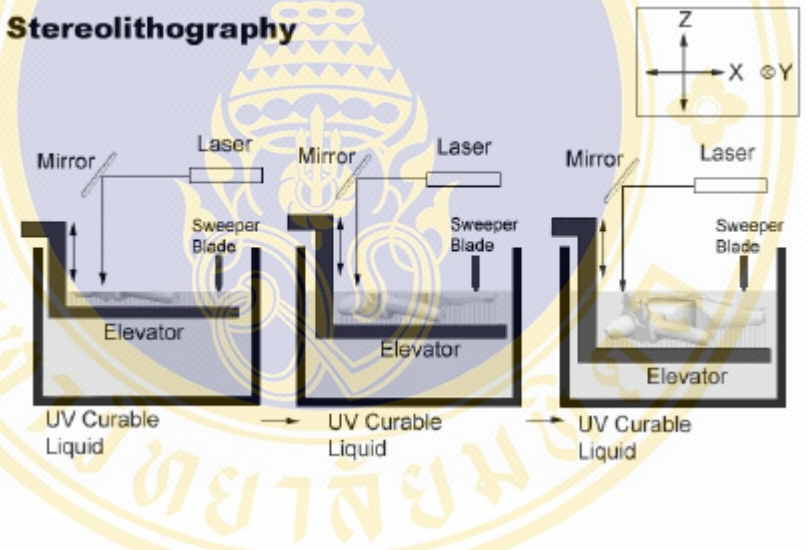

Figure 2.3 Schematic diagram of the SLA process [10]

2.1.4.2 Selective Laser Sintering (SLS)

Selective laser sintering creates three-dimensional objects by heating and fusing powder materials. Laser-sintering machines build each layer by first spreading a shallow layer of powder onto a building platform. Then, a laser (a carbon dioxide laser) selectively fuses powdered material by scanning cross-sections generated from a 3D digital description of the part. The building chamber is heated to just below the melting temperature of the powdered material so that a slight amount of energy from the laser will sinter the powder grains. Everywhere the laser touches, its energy heats the powder grains, causing them to adhere to their neighbors. Once a layer is

completed, the building platform, which is mounted on a moveable piston, lowers by one layer's thickness and a new layer of loose powder is spreaded across the top of the growing part. The process is repeated until the part is completed.

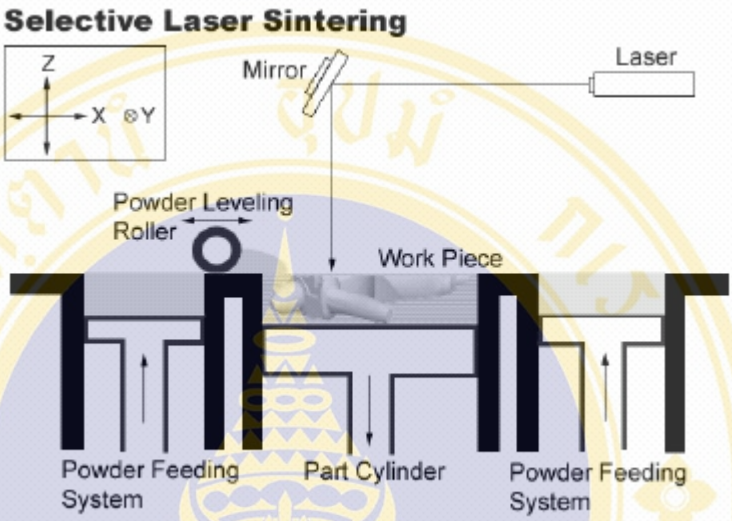

Figure 2.4 Schematic diagram of the SLS process [10]

Parts built by laser sintering do not require supports. The unsintered powder surrounding previous layers supports isolated or overhanging areas of a layer as it is built. When finished, a sintered part is encased in loose powders. The advantage of laser sintering is the wide range of powder materials can be processed. Any material that can be powdered and melted might be used, for example polycarbonate, nylon, or glass-filled nylon, polyamide, acrylic-based polymer, elastomeric polymer, zirconium and silica sands, and polymer-coated steel and metal-alloy powders [10,13,14].

2.1.4.3 Laminated Object Manufacturing (LOM)

The laminated objects manufacturing method was developed by Michael Feygin of Helysis [12]. LOM creates objects from bonding layers of laminate material together. Raw material is usually a paper sheet laminated with adhesive on one side, but plastic and metal laminates are also used. The laminated material is supplied on a roll. It passes up over a vertically moving table to a take-up reel. At the start of each layer, a heated roller passes over the newly exposed sheet of material causing it to adhere to the previous layer. The laser then traces out the outline of the layer. Non-part areas are cross-hatched to facilitate removal of waste material [15]. Materials of varying thickness can be used.

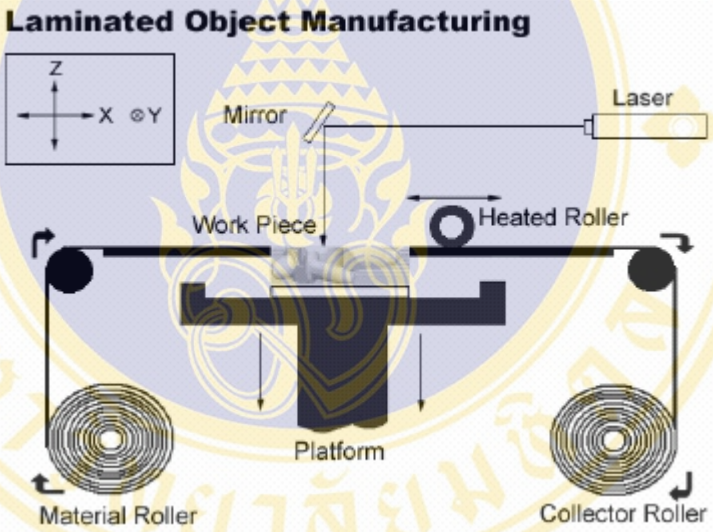

Figure 2.5 Schematic diagram of the LOM process [10]

Once the laser cutting is completed, the platform moves down and out of the way so that fresh sheet material can be rolled into position. Once new material is in position, the platform moves back up to one layer below its previous position [13,16].

2.1.4.4 Fused Deposition Modeling (FDM)

Fused deposition modeling process was developed by Stratasys Inc.[17]. The FDM technology extrudes a thin semi-molten plastic filament and deposits it layer by layer to build an object. The machine heats plastic to a temperature just below its melting point. The platform is maintained at a lower temperature, so that the thermoplastic quickly hardens.

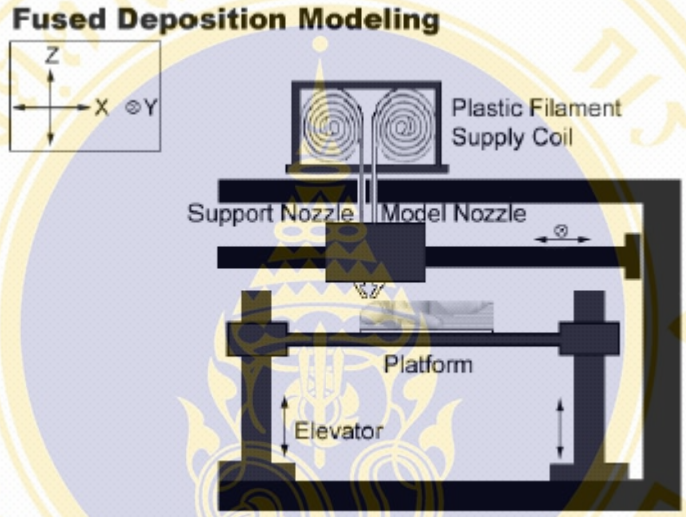

Figure 2.6 Schematic diagram of fused deposition modeling [10]

The materials which can be used in FDM machine include polyester, polycarbonate, polyphenylsulfone, acrylonitrile butadiene styrene (ABS), elastomers, and investment casting wax [10,18]. An FDM machine enables full desktop operation and is fully suitable for use in an office environment.

2.1.4.5 Three Dimensional Printing (3DP)

Three dimensional printing (3DP) employs inkjet technology. It was developed by MIT in the late 1980s [19]. The 3D printer, produced by Z Corporation of Burlington, MA is an example of this technology. Desktop printers from Z Corporation employ two basic material systems, either a plaster or starch-based powders. The faster and less expensive is a starch-based powder. A plaster-based powder can be used for building more durable parts.

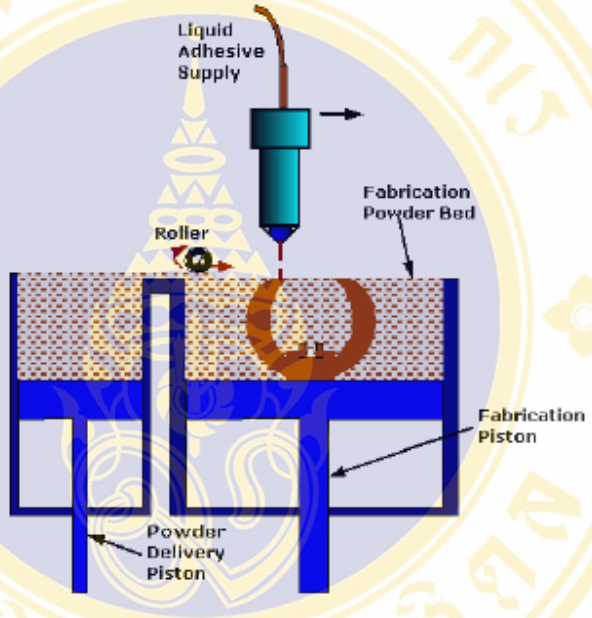

Figure 2.7 Schematic diagram of three dimensional printing [20]

As similar to other rapid prototyping systems, the input for three dimensional printing is a graphical file that has been converted into standard STL format. Software in the 3DP system slices the STL model into a series of horizontal cross sections. The process starts by depositing a layer of powder material at the top of a fabrication chamber. To accomplish this, a measured quantity of powder is first dispensed from a similar supply chamber by moving a piston upward incrementally. Next, a thin layer of powder (between 0.076 mm. and 0.254 mm. thick is spreaded by a roller onto a platform mounted on a piston in a building box. Inkjet printhead sweeps across the surface of the layer and print the image of a single cross section onto the powder. Where the binder is printed, the powders are glued together. Once a layer is complete, the piston lowers the build platform by one layer thickness and the process is repeated

until the entire object is formed within the powder bed. Loose powders surrounding the printed area remain in place and support the part as it is built. When a part is finished, the piston raises the build platform and excess powders can be brushed or vacuumed off the part. Objects must usually be infiltrated with an infiltrant before they can be handled without much risk of damage. Once infiltrated, they can be polished to achieve a smooth surface. Completed prototypes are said to have very fine detail and excellent surface finish [19-22].

Table 2.1 RP Technologies Comparison Table [23]

Technology	**SLA**	**SLS**	**FDM**	**3DP**	**LOM**
Vendor	3D system	3D system	Stratasys	Z Corporation	Cubic Technologies
Maximum part size (inches)	20x20x24	15x13x18	24x20x24	20x24x16	32x22x20
Speed	average	fair	poor	excellent	good
Accuracy	very good	good	fair	fair	fair
Surface finish	very good	fair	fair	fair	Fair to poor
Strengths	large part size, accuracy	accuracy, materials	office OK price, materials	speed office OK price, color	large part size, good for large castings, material cost
Weaknesses	post processing, messy liquids	size and weight, system price, surface finish	speed	limited materials, fragile parts	part stability, smoke finish and accuracy
System Price	$75,000-800,000	$300,000	$30,000-300,000	$30,000-70,000	$120,000-240,000
Material Cost ($/pound)	$75-110 (Plastic)	$30-60 (Plastic) $25-30 (Metal) $5 (Foundry sand)	$115-185 (Plastic)	$0.35 / cu in (Starch) $0.60 / cu in (Plaster)	$9 (Plastic) $5-8 (Paper)

2.2 Medical Applications of Rapid Prototyping

Rapid prototyping has been used in medical applications ranging from the design and building of medical implants and devices to a pre-operative planning tool for surgeons. In couple with two distinct technologies, namely medical imaging and computer graphics, quick and accurate rapid prototyping models can be produced for a variety of purposes.

2.2.1 Medical models

The most common application of rapid prototyping technology in the medical field is as a pre-operative planning tool. A model of an impaired or defective area is built which can be used in patient education and physician training [24]. These models serve as planning aids for surgeons who can use them to determine the most effective and safest approach prior to surgery. They give medical staff an understanding of the shape (real touch), orientation, relative location and size of internal anatomical structure.

In orthopedic surgery, different colors can be used to highlight critical structures within a single RP model. This might be used to show the extent of an invasive tumor that is spreading within a bone. Stereolithography is often the rapid prototyping method of choice for these applications [4]. The transparency of the model and recent developments in color resins allow distinct visualization of tumors or other anomalies within the surrounding tissue or bone. Another possibility is to manufacture the model in several separate parts, corresponding to bone fragmentation, in order to study their re-assembly. For example, SLA was used to produce a model of a pelvis with a severely fractured acetabulum resulting from a fall [25]. The extent of multiple fragmentation cannot be understood from a 2D x-ray photographs. It is estimated that operating time is cut in half when physical models are used as planning aids, particularly for rare and delicate procedures [4,25].

Rapid prototyping model has also been used in cranio-maxillofacial applications [26-27]. Three-dimensional models can be constructed from CT scans in order to model maxillofacial deformities. The use of pre-operative planning model by color stereolithography is useful in ablative surgery of the maxilla and the ethmoid

bone [28]. The colouring of the tumour clarifies its relation to surrounding structures such as the sinuses, the orbit, the infratemporal fossa and intracranial space.

2.2.2 Prostheses and Implants

It was recognized quite early that rapid prototyping could bring great improvements to the fields of prosthetics and implantation. In general, hip replacements and other similar surgeries were carried out using standard-sized replacement parts. This works satisfactorily for some types of procedures, but not all cases of any given procedures. There are always patients outside the standard range. Rapid prototyping can be used to manufacture a custom prosthesis that precisely fits a patient. In hip replacement, CT scan data from a patient, is combined with engineering data such as standard geometries to connect to the bone. Then, a model of an optimally fitting joint is produced using rapid prototyping technology. The model is then used as a casting pattern to manufacture a customized titanium implant. Moreover, rapid prototyping can be used in combination with conventional casting process to produce ceramic and metal implant [3,29]. A negative mould is built via RP which is then used to cast molten metal into a desired shape. Clinical success has been reported with Co-Cr-Mo knee femoral components fabricated by this approach.

There are many applications of rapid prototyping in cranio-maxillo facial surgery. Custom made implants for large cranium defect have already been described by many authors [4]. Most authors describe the design and the manufacturing of the implants using stereolithographic models of cranial structures [4,30]. The concerned implants are designed to cover a known defect after a trauma or an undefined defect before the tumor removal. Moreover, an innovative cranioplasty technique with PMMA has been proposed [31]. 3D model of the prosthesis is designed using computed tomography, Materialise MIMICS and professional CAD equipment (Fig 2.8), and then manufactured using a rapid prototyping process which allows automatic modeling of a customized prosthesis prior to surgery. Preformed prostheses result in superior cosmetic compared to intraoperatively-constructed prostheses. Completion of the PMMA polymerization process prior to surgery significantly reduces inflammatory risk. Cost saving may be attributed to shorter operating times, reduced incidence of infection and improved mechanical precision and process.

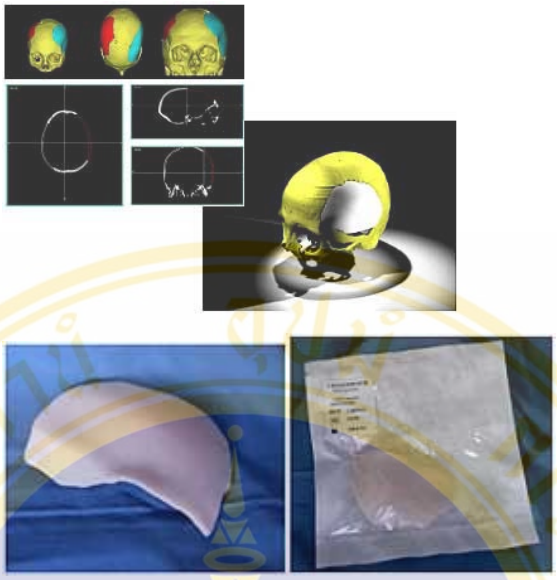

Figure 2.8 An innovative cranioplasty technique with PMMA [31]

2.2.3 Tissue Engineering Applications

There are many researches of using rapid prototyping in bone tissue engineering. Plasti-Bone™, an experimental technique developed jointly by Advanced Ceramics Research, Inc. (ACR) and the University of Arizona (UA) for the Office of Naval Research, uses rapid prototyping technique to create custom artificial bone grafts (Polymer/Ceramic Materials) designed to help damaged bone portions. This innovative technology has major implications for reconstructive surgery for wounded soldiers exemplified by the fact that RP allows for custom implants to be crafted on the battlefield [32-33]. In addition, rapid prototyping and especially 3D printing is well suited to generate complex-shaped porous ceramic matrices directly from powder materials. A new process chain for custom-made three-dimensional porous ceramic scaffolds for bone replacement with fully interconnected channel network for the repair of osseous defects from trauma or disease has been reported. [33-34]

In complex craniofacial reconstruction, integrated image-based design and RP technology can create scaffolds that attain desired elasticity and permeability while fitting any 3D craniofacial defect [35]. The scaffolds could be manufactured from degradable polymers, calcium phosphate ceramics and titanium. The designed scaffolds supported significant bone regeneration for all pore sizes ranging from 300

to 1200 microns which are clinically applicable for complex craniofacial reconstruction.

2.2.4 Other RP Applications in Medicine

While the major medical applications of RP technology are related to surgery, there are other applications with the potential to significantly improve health care industry. Recent application has been applied for drug delivery systems. 3D Printers for making drug delivery systems are already commercialized and it can produce up to 20,000 tablets per hour. According to Sharke [36], the local composition control capability of 3D Printers (also used for making functionally graded materials) means that the drug dosage can be controlled accurately. Alternate layers of powder can be of different material, thereby controlling the drug release time by adding inert materials. Therics, Inc. of NYC is using RP technology to develop pills that release measured drug doses during the day and other medical products [37].

The other application is organ printing [36]. Mironov *et. al*. [38] reported some research in this direction. They developed a printer that can print gels, single cells and cell aggregates into a 3D gel. Their process consists of three stages: pre-processing (creating a CAD modelling which can be from scanned data), processing (printing) and post-processing (perfusion of printed organs and their biomechanical conditioning). However, no human or animal testing is reported. Yan *et. al*. [39] are doing similar research.

2.3 Medical Rapid Prototyping Process

2.3.1 Medical Model Fabrication

The medical modeling process can be broadly split into three areas: data acquisition, image processing and model production.

Data acquisition: The process starts with 3D data of internal and external human body structures which are acquired from Computer Tomography (CT) for bone structure or Magnetic Resonance Imaging (MRI) for soft tissue. Other medical imaging systems which can be used include Ultrasound System, Mammography and X-ray. The data are normally presented as a slice format, showing cross-sections of the patient [5, 40].

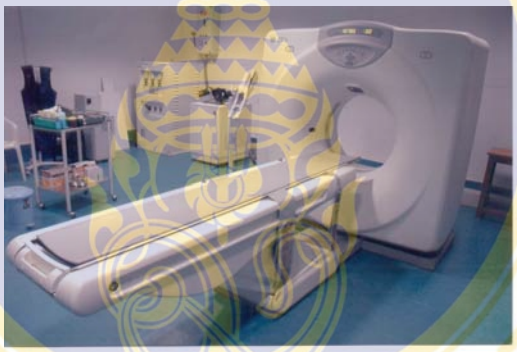

Figure 2.9 Computer Tomography (CT) machine [41]

Image processing: To generate the reconstructed computer model, the patient's image data must be processed to identify and extract the relevant structures corresponding to the region of interest (image segmentation). This is done by breaking the 3D computer model into series of slices of a finite thickness. The contours for each slice are interpolated to form a completed 3D image. A number of software packages have been developed to enhance the visualization of 3D computer models and are commercially available. Some of these software packages include Analyze biomedical image processing package [42], Surgicad Template from Surgicad Corp. and Intergraph Corp. and Mimics from Materialise Software Company [43]. When segmentation is completed, the data can be translated to machine instructions that can be understood by all RP machines. The standard interface from CAD to RP is the Standard Triangulation Language (STL).

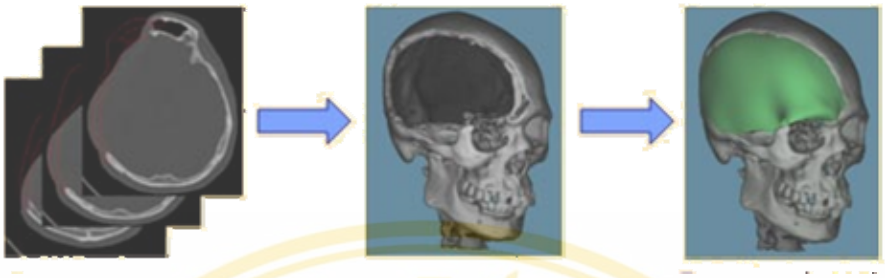

Figure 2.10 3D Reconstructed computer model [44]

Model production with RP: After machine instructions are transferred to rapid prototyping machine, the building can start. RP machines build one layer at a time from polymers, paper, or powdered metal. When building is finished, supporting structures are removed and the model is cleaned, or post-processed.

Figure 2.11 Medical model from RP [44]

2.3.2 Implant fabrication from medical model (Indirect fabrication)

Since most RP processes cannot fabricate biomedical materials directly, the desired biomaterial such as PMMA has to be molded from a RP model. The RP model is employed as patterns of the desired implants to create silicone or plaster moulds for further casting by biomedical materials [40].

Mold cavity biomedical implant

(a) (b)

Figure 2.12 Biomedical implant molded from a RP model

Fig.2.12 showed an impression of the RP model on two opposing plaster casts. When the RP model is removed, the resultant cavity can then be filled with biomedical materials.

Polymethyl methacrylate, which is abbreviated as PMMA, is well known by a variety of trade names for example Lucite (INEOS Acrylics,Inc.) and Plexiglas (Atofina Chemicals.Inc.) [45]. In bony reconstruction of skull defects, it can be used as a facial contour implant [46]. PMMA does not adhere to bone and fixation is done by mechanical interlock. It can be purchased in preformed implant form, or in a self-curing form. The self -curing form comes as two components, a liquid monomer and a polymethyl methacrylate powder. These are mixed together and a polymerizing reaction takes place creating a temporarily mixture that can be shaped and trimmed to fit the needs of the surgeon. There is also the risk of side effects due to the toxicity of the monomeric component [45-46] although this is rarely observed. Nevertheless, it has excellent qualities such as superior biocompatibility and tissue ingrowth promoted by drilling multiple holes in the implant. The preformed version can be cut and shaped with rotary burrs.

2.4 Biomaterials for 3DP Machine Used in This Study: Properties and Biocompatibility

2.4.1 Polymethyl methacrylate

Polymethyl methacrylate (PMMA), more commonly known by the generic name acrylic, is polymerized from the methyl methacrylate monomer. It is a vinyl polymer which can be produced using a variety of polymerization mechanisms. The most common technique is the free radical polymerization of MMA (Fig.2.13) [47].

PMMA is a hard material and is extremely clear because of the amorphous arrangement of its molecules. It has long been used by orthopaedic surgeons as bone cement for joint replacement or implant to replace a skull bone defect.

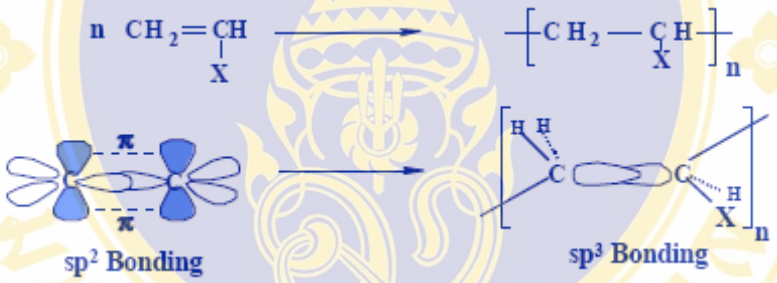

Figure 2.13 Chain polymerization for an acrylate system [47]

Properties

Polymethyl methacrylate is an amorphous plastic with a high surface gloss, a clear transparency of 92 % (inorganic glass also has a transparency of 92 %), and a refractive index of 1.49. PMMA is classified as a hard, rigid, but brittle material with a glass transition temperature of 105°C [48]. The typical technical data is shown in table 2.2.

Table 2.2: The physical and mechanical properties of PMMA (acrylic denture base materials) [49]

Density (g/cm^3)	1.16-1.18
Melting Temp. Range (°C)	220 - 240
Water sorption (mg/cm^2) , ADA Test	0.69
Water solubility (mg/cm^2)	0.02
Tissue compatibility	Good
Shelf life	Powder and liquid,good; gel,fair
Tensile Strength (MPa)	48.3 – 62.1
Compressive Strength (MPa)	75.9
Elongation at break (%)	1-2
Elastic Modulus (GPa)	3.8

PMMA has good mechanical strength, acceptable chemical resistance, and extremely good weather resistance. Other properties include a high Young's modulus and good hardness with low elongation at break. PMMA is one of the hardest thermoplastics and is also highly scratch resistant. It is viscoelastic and stronger in compression than in tension and shear. The fatigue strength is approximately 20-25% of the single cycle strength. PMMA has favorable processing properties, good thermoforming, and can be modified with pigments, flame retardant, UV resistant additives and scratch resistant coatings [47,50].

Biocompatibility of PMMA

Biocompatibility is the ability of a material to perform with an appropriate host response in a specific application [51-52]. PMMA is biocompatible and stable in the body. Allergic reactions are seldomly seen. Residual monomer is about 0.3% [53].

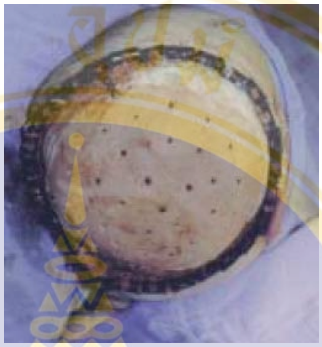

Figure 2.14 Per-operative view of the PMMA implant [52]

Intraocular lens (IOL) implantation also use PMMA. It is the standard material for use in IOL manufacturing. It was the first material to be used and has withstood the test of time as the majority of IOLs implanted worldwide today are still made of it. PMMA benefits from inducing a minimal intraocular inflammatory reaction [54]. Moreover, PMMA can be used as the material to produce biocompatible hollow-fibre dialyzers. Toray PMMA hollow fibres for artificial dialysis were put on the market in 1973 [55].

2.4.2 Dextrin

Dextrin is a glucose-containing saccharide polymer linked by α-(1-4)D-glucose units and is produced by partial hydrolysis or roasting of starch [56-57]. Dextrins differ from other modified starches in that, not only are they reduced in viscosity, but they also have appreciable cold water solubility and reduced tendency to gel [57]. Dextrins are often used as an ingredient in adhesives or binders. As adhesives, dextrins are used in making all types of paper products (bags, laminates, paper boxes, paper tubes and envelopes). Dextrins also can be used in adhesives and coatings that come into contact with food products. Besides adhesives, they are also used in other industries including the foundry, agricultural, and various arts and crafts applications. The role of dextrins in foundries is well-known. The main function is to give good green strength to moulds and to prevent deformation of the core before being fired in the furnace. Another important point is that dextrins do not make the core too dense, so that there are no trapped gases which cause blow holes. All these advantages make dextrins very good as core binding materials.

Properties

Unlike starch, dextrins are soluble in water. The severity of the heat and acid treatment determines the degree of solubility, which is the basis for classifying or grading dextrins. Finished dextrins are very fine powder varying in colour from pure white to light yellow. The typical technical data is shown in table 2.3.

Table 2.3: The physical properties technical data of dextrin [58]

	White	**Yellow**
Moisture (max.)	10%	10%
Ash (max.)	0.40%	0.05%
pH	2.5 to 3.5	2.5 to 3.5
Reducing sugar	6 to 8%	3 to 5%

Biocompatibility of Dextrin

Because of the biocompatibility and degradability of starch-based materials, dextrin might be suitable for biomedical applications [56]. Dextrin, which is used in this experiment is maltodextrin. Maltodextrins are generally recognized as safe (GRAS) food ingredients. They can be used in pharmaceutical and food products [59].

2.4.3 Polyvinyl alcohol

Polyvinyl alcohol (PVA) is polymer that is often used for various pharmaceutical and biomedical applications [60]. It is a good binder for the solid particles including pigments, ceramics, cement and textile fibers. It is obtained by alcoholysis with methanol of polyvinyl acetate [61]. The molecular formula of it is $[-CH_2CHOH-]_n$. It has a melting point of 230 °C and 180-190 °C for the fully hydrolysed and partially hydrolysed grades respectively. PVA also decompose rapidly above 200 °C. This polymer offers outstanding resistance to oil, grease and solvents, high tensile strength, flexibility, and high oxygen barrier. PVA is a water-soluble synthetic polymer with excellent film-forming, emulsifying, and adhesive properties. Commercial PVA grades are available with high degree of hydrolysis (above 98.5%). Its solubility in water depends on its degree of polymerization and degree of hydrolysis [62].

In addition, polyvinyl alcohol is one of the few truly biodegradable synthetic polymers. The degradation products are water and carbon dioxide. Biodegradation of PVA depends on the microbe population of the aqueous or soil environment. Decreasing the molecular mass of PVA also increases the biodegradation. Temperature is another important criterion for biodegradation of PVA. Biodegradation of PVA can also be improved by adding natural components like starch, cane sugar or protein.

Biocompatibility of PVA

PVA have certain advantages that make them excellent candidate for biomaterials [63]. Some of these advantages include their non-toxic, non-carcinogenic and bioadhesive characteristics. PVA gels exhibit a high degree of swelling in water (or biological fluids) and a rubbery and elastic nature. These properties make them simulating natural tissue and can be accepted in the body. Oka *et. al.* [64] investigated PVA gels for the development of articular cartilage. They reported the biocompatibility as well as the mechanical properties of PVA gels in relation to their usefulness as artificial articular cartilage. Series of *in vivo* tests was performed in an intra-articular environment. It was found that upon implantation of the material into the rabbit knee joint, there was only slight to mild inflammation initially. It was found to have excellent biocompatibility for use as an artificial articular cartilage.

CHAPTER III
MATERIALS AND METHODS

3.1 Materials

Polymethyl methacrylate was purchased from Lang Dental., Ltd., USA. Materials used as binder are maltodextrin (Shandong Duqing, Inc., China) and polyvinyl alcohol (Sigma-Aldrich, USA). These materials were supplied in the form of powders with particle size ranging 80-100 microns. Infiltration resin used is heat-cured dental acrylic based on mixture of triethylene glycol dimethacrylate, (2,2-bis[4(2-hydroxy-3methacryloyloxypropyloxy)-phenyl] propane and urethane dimethacrylate).

3.2 Experimental Procedures

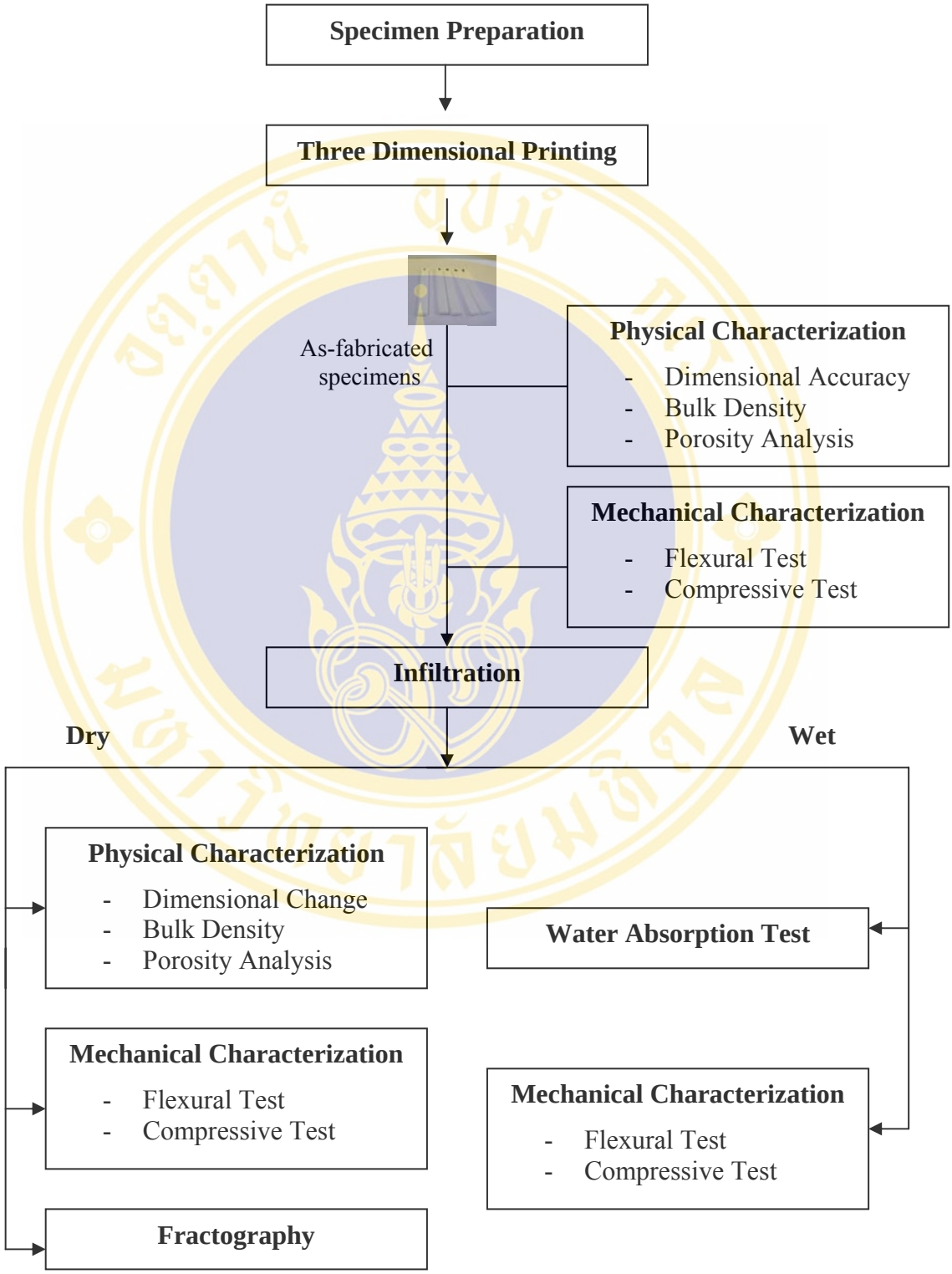

Figure 3.1 Diagrammatic representation of the research process

3.2.1 Specimen Preparation

Various blends of materials were formulated in order to adjust the properties of the specimens by varying individual composition. Each formulation was prepared by initially stirring in a plastic bag and then thoroughly mixed by a mechanical blender. An equal amount in mixture of 50% PMMA and 50% binder was first prepared. It was then printed by three dimensional printing machine (Figure 3.2). From the observation, the ratio of the mixture was decreased or increased as shown in Table 3.1. Binder content greater than 60% was found to yield high shrinkage specimen with curvature. Binder content lower than 10% was too weak for specimen handling.

Figure 3.2 Three-dimensional printing (3DP) machine
(Z400 system, Z Corporation, USA)

Table 3.1 Materials formulation

Formulation	PMMA (%)	Maltodextrin (%)	PVA (%)
1	40	50	10
2	50	40	10
3	60	30	10
4	70	20	10
5	80	10	10
6	90	0	10

Rectangular bars (80 mm. x10 mm. x4 mm) and cylindrical objects (Ø10 mm. X 20 mm.) were fabricated as shown in Figure 3.3. A layer thickness of 0.175 mm. and water was used as a binding liquid in all formulations.

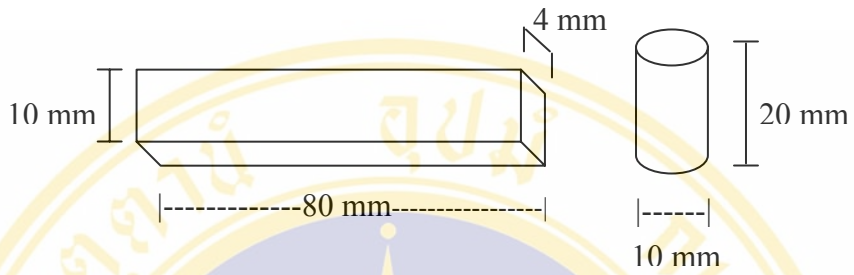

Figure 3.3 Rectangular bar and cylindrical specimen

3.2.2 Infiltration

Infiltration material in this study is heat-cured acrylic. Prior to infiltration, the specimens were dried at 75 °C for 15 minutes. They were then dipped into the resin bath to let the resin diffuse into the specimens naturally. They were cured at 105°C for 30 minutes and post-cured at 120°C for 30 minutes.

3.2.3 Characterizations

3.2.3.1 Dimensional Accuracy

Dimensions in width, thickness and length of green structure fabricated by 3DP machine were measured by a vernier caliper (Mitutoyo) with the reading resolution of 0.01 mm. and recorded. The measured dimensions were compared with the setting dimensions from 3DP machine to determine the accuracy. Dimensions of green structures were compared with those of infiltrated structures to determine dimensional change. Dimensional error and dimensional change were calculated by following equations:

$$X_e = \left(\frac{X_m - X_0}{X_0} \right) \times 100 \quad \text{..... Equation 3.1}$$

$$X_d = \left(\frac{X_2 - X_1}{X_1} \right) \times 100 \quad \text{..... Equation 3.2}$$

Where X_e is a dimensional error (%)

X_m is a measured dimension (mm)

X_0 is a setting dimension (mm)

X_d is dimensional change(%)

X_2 is a dimension after infiltration (mm)

X_1 is a dimension before infiltration (mm)

3.2.3.2 Bulk Density Determination

Volume was calculated by multiplying width, thickness and length which were measured by a vernier caliper (Mitutoyo) with the reading resolution of 0.01 mm. The weights of specimens were measured by a digital balance (Mettler Toledo PB4002-S) with the reading resolution of 0.0001 grams. Bulk density was then calculated by dividing the weight by the volume as following equation:

$$D = m / v \quad \text{Equation 3.3}$$

Where D is a bulk density of specimen (Mg/m^3)

m is a weight of specimen (Mg)

v is a bulk volume of specimen (m^3)

3.2.3.3 Porosity Analysis

Apparent density of samples was measured using the gas displacement techniques by gas pycnometer (Ultrapycnometer 1000, Quanta Chrome, USA). Porosity was calculated by following equation:

$$P = \left(\frac{\rho_a - \rho_b}{\rho_a} \right) \times 100 \quad \text{Equation 3.4}$$

Where P is a porosity of specimen (%)

ρ_a is an apparent density of specimen (Mg/m^3)

ρ_b is a bulk density of specimen (Mg/m^3)

3.2.3.4 Flexural Test

The mechanical property was investigated using three-point bending method based on ASTM D790. Flexural tests were performed on universal testing machine (Instron 55R,USA) with a 10 kN load cell. The rectangular beam (80 mm. x10 mm. x4 mm.) was placed between two metal supports. The span length was set at 64 mm. The crosshead speed is 1.9 mm/min. All flexural tests were performed at 23 °C and 50% R.H..

Figure 3.4 Flexural test configuration

3.2.3.5 Compressive Test

Compressive test was performed on cylindrical specimens (Ø10 mm. X 20 mm.) using a universal testing machine (Instron 55R, USA). The specimen was placed between two parallel platens according to ASTM D695. Specimen was compressed at a constant rate of 1.3 mm/min. All tests were performed at 23°C and 50% R.H..

Figure 3.5 Compressive test configuration

3.2.3.6 Water Absorption

Prior to the test, the specimens were dried in an oven at 75°C for 15 min and then placed in a room environment to cool. Immediately upon cooling, the specimens are weighed. The material is then submerged in water at 23°C for 24 hours according to ASTM D570. When the time was reached, specimens are removed, patted dry with tissue paper, and weighed. Water absorption is calculated by following equation:

$$\text{Water Absorbtion}(\%) = \left[\frac{\text{Wet weight - Dry weight}}{\text{Dry weight}}\right] \times 100 \quad \text{.....Equation 3.5}$$

3.2.3.7 Fractography

Fractured surfaces of tested specimens were observed by a scanning electron microscope (JEOL JSM-6301F, Japan). The specimens were gold sputtered prior to the test. The accerating voltage was 10 kV.

CHAPTER IV
EXPERIMENTAL RESULTS

The experiments were divided into two parts, which were as-fabricated samples and infiltrated samples. The properties of the infiltrated samples were also compared with the properties of polymethyl methacrylate which was indirectly fabricated by conventional method.

4.1 As-fabricated Samples

4.1.1 Dimensional Accuracy

The average dimensional errors of as-fabricated samples compared to the designed computer graphic are shown in Table 4.1 and Figure 4.1. The error in width of samples tended to decrease with decreasing binder content whereas the error in length increased. The errors in thickness were fairly constant for all formulations. Overall errors were found to be less than 6%.

Table 4.1 Percentage of dimensional error of as-fabricated samples

Formulation	Binder content (%)	Dimensional error (%)		
		Width	Length	Thickness
1	60	-5.70±1.03	0.71±0.71	1.40±2.75
2	50	-4.78±1.17	0.99±0.29	3.43±2.55
3	40	-4.72±1.20	0.57±0.23	1.43±3.88
4	30	0.21±0.80	1.88±0.34	3.80±1.06
5	20	0.97±0.75	2.37±0.21	5.16±1.28
6	10	0.37±0.12	3.14±0.04	2.42±0.58

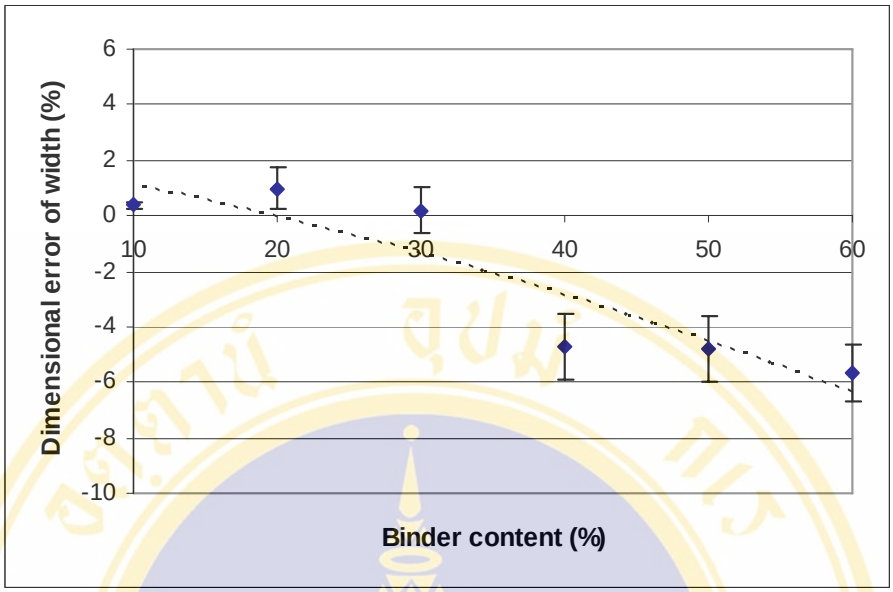

(a)

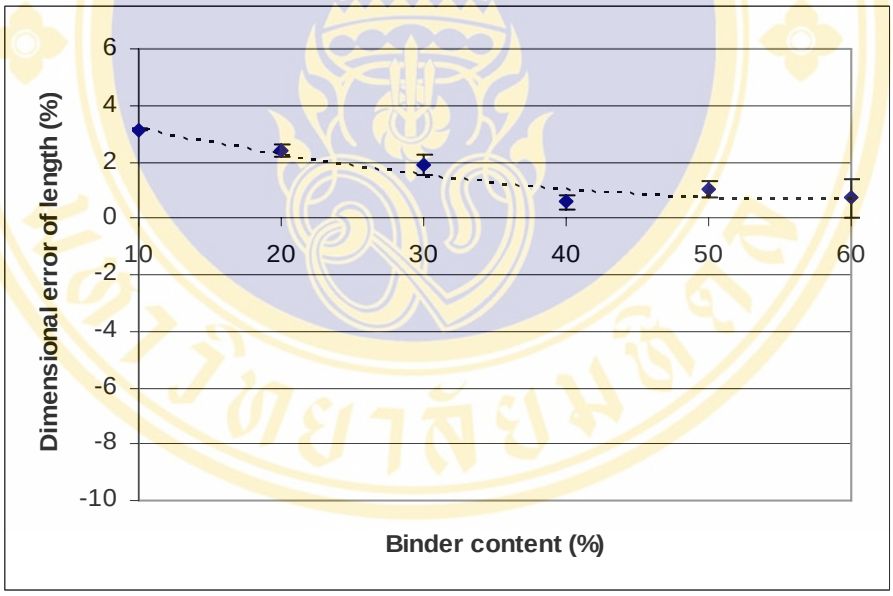

(b)

Figure 4.1 Percentage of dimensional error in (a) width, (b) length and (c) thickness

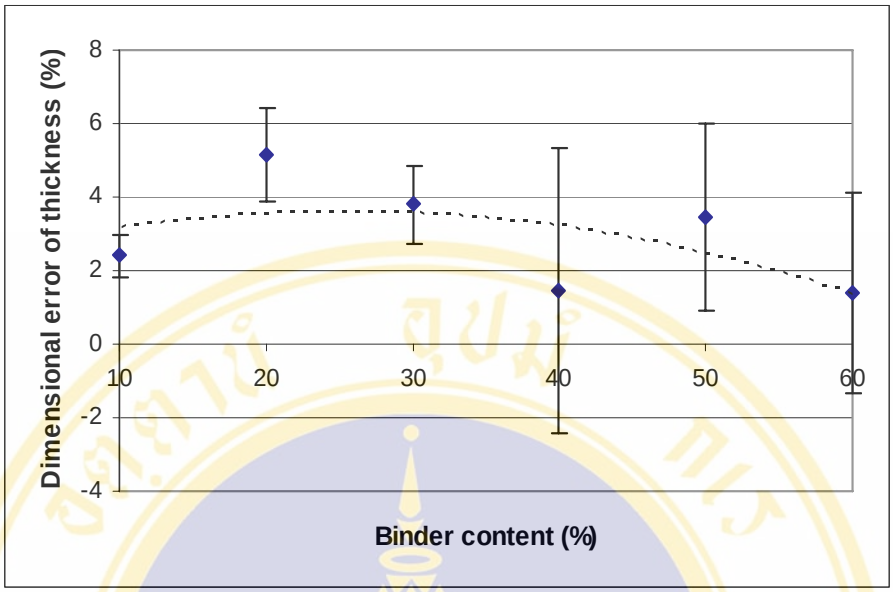

(c)

Figure 4.1 Percentage of dimensional error in (a) width, (b) length and (c) thickness (Cont.)

Figure 4.2 shows overall view of the percentage of dimensional error. The results showed that dimensional errors were low when the binder content was less than 30%.

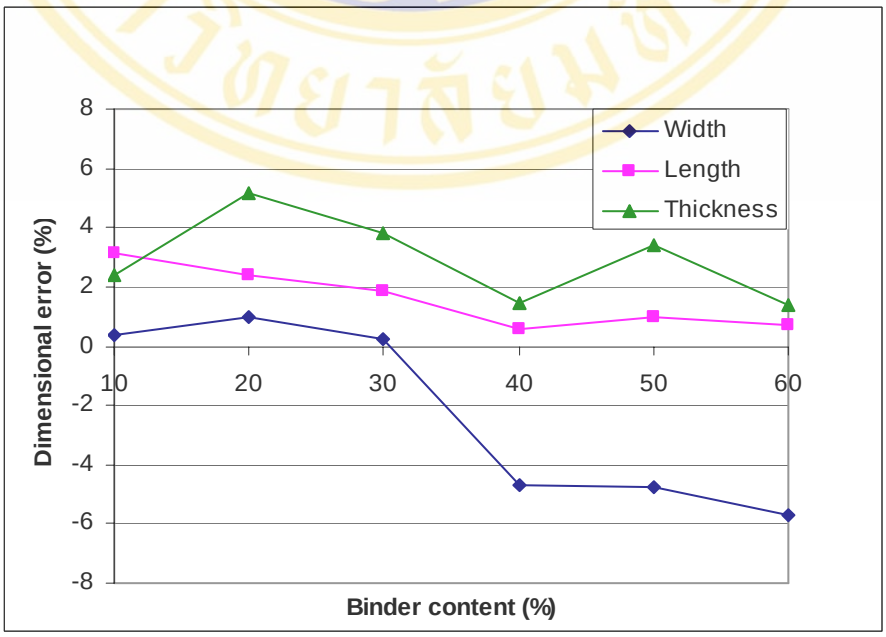

Figure 4.2 Percentage of dimensional error of various formulations

All formulations in this study were able to be fabricated by 3DP machine, however, formulation 6 (0% dextrin,10% PVA) was very fragile. Therefore, this formulation was discarded from further characterizations.

4.1.2 Density and Porosity

The results indicate that increasing binder content slightly increase bulk density but decrease the percentage of porosity in the samples (Table 4.2 and Figure 4.3-4.4).

Table 4.2 Density and porosity of as-fabricated samples

Binder content (%)	Bulk density (Mg/m^3)	Porosity (%)
60	0.7087±0.03	41.57
50	0.7515±0.02	48.98
40	0.6929±0.02	51.60
30	0.6539±0.03	55.80
20	0.6017±0.02	57.19

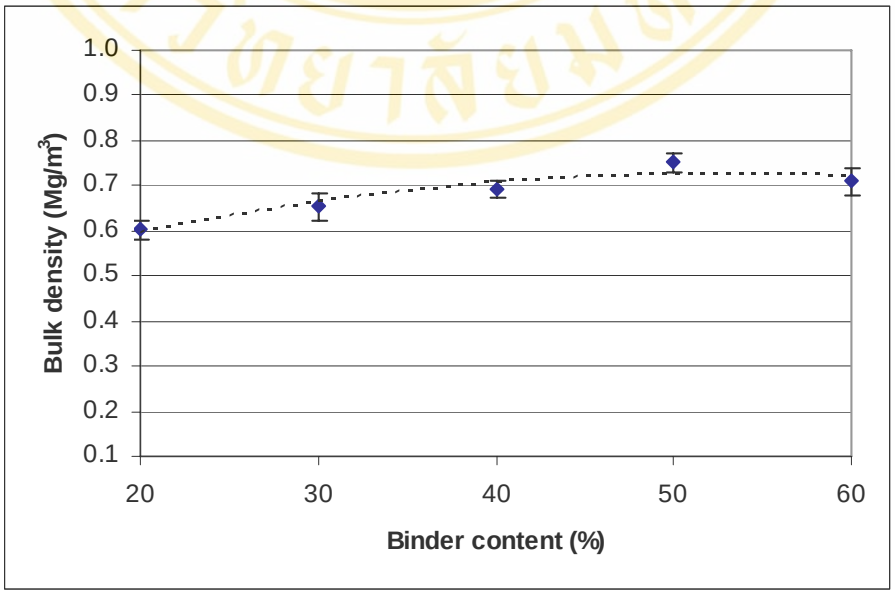

Figure 4.3 Bulk density of various formulations

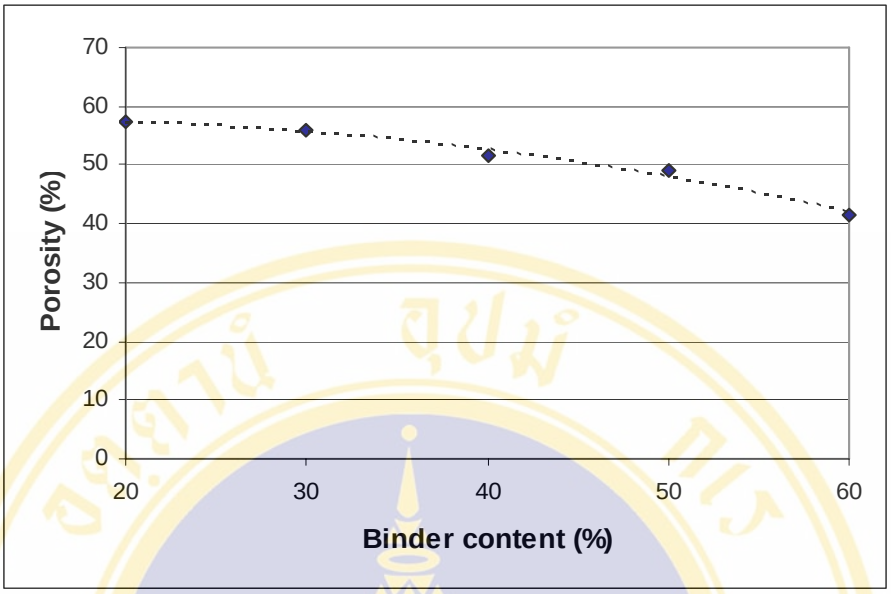

Figure 4.4 Porosity of various formulations

4.1.3 Mechanical Properties

The mechanical properties of as-fabricated samples are presented in Table 4.3. The flexural strength and flexural modulus was found to increase with increasing the amount of binder, but the flexural strain at break decreased slightly when the amount of binder increased (Figures 4.5-4.7).

In the case of compressive properties, the results show that compressive strength and compressive modulus increases with increasing binder content, but compressive strain at break decreased slightly when the amount of binder increased similarly to flexural properties (Figures 4.8-4.10).

Table 4.3 Mechanical properties of as-fabricated samples

Binder content (%)	Strength (MPa)		Modulus (GPa)		Elongation (%)	
	Flexural	Compressive	Flexural	Compressive	Flexural	Compressive
60	1.16±0.13	4.35±0.56	0.36±0.05	0.38±0.07	0.47±0.02	4.02±0.78
50	0.87±0.15	3.76±0.99	0.20±0.01	0.27±0.04	0.57±0.03	7.60±0.83
40	0.44±0.21	1.88±0.18	0.13±0.01	0.16±0.01	0.48±0.02	4.59±0.99
30	0.32±0.03	0.42±0.06	0.08±0.00	0.03±0.01	0.61±0.03	4.67±0.57
20	0.20±0.04	0.20±0.03	0.04±0.00	0.01±0.00	0.65±0.03	6.75±0.30

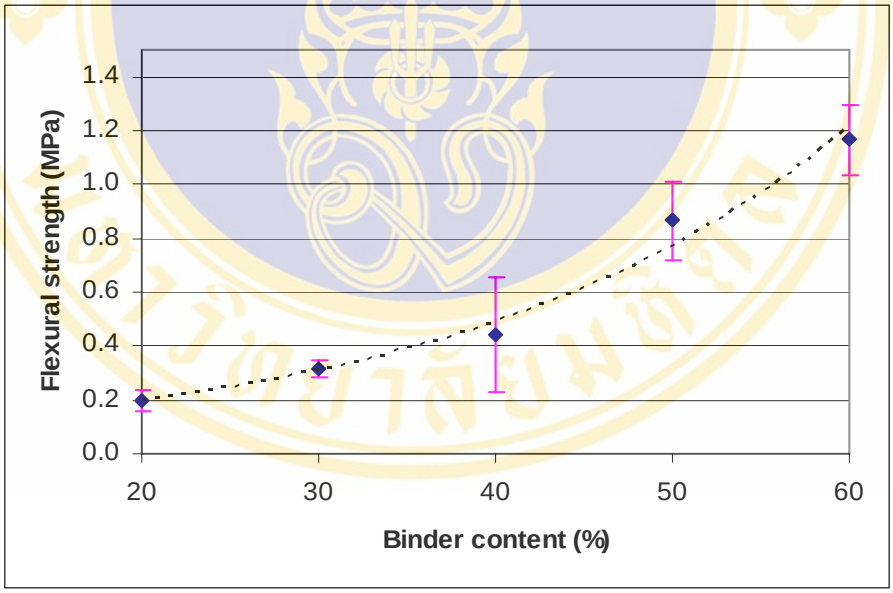

Figure 4.5 Flexural strength of as-fabricated samples

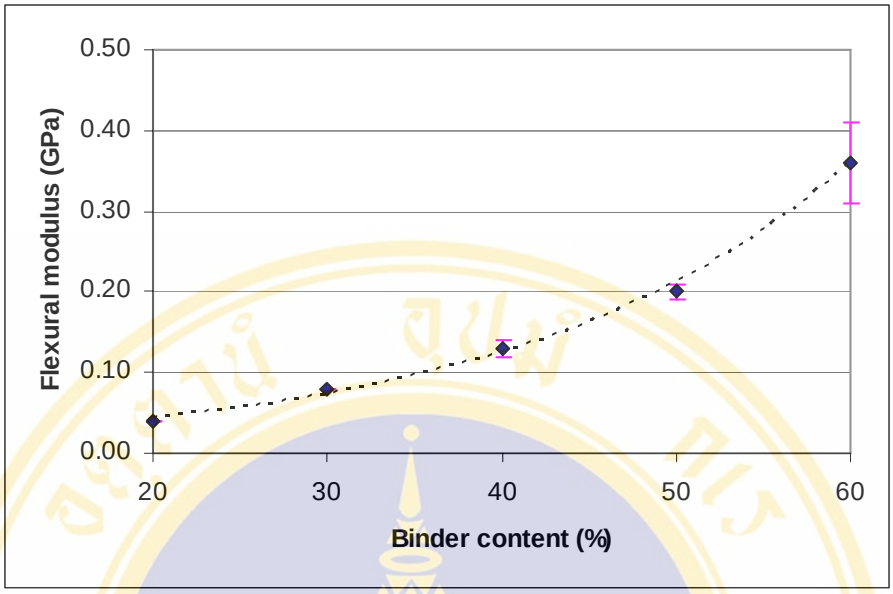

Figure 4.6 Flexural modulus of as-fabricated samples

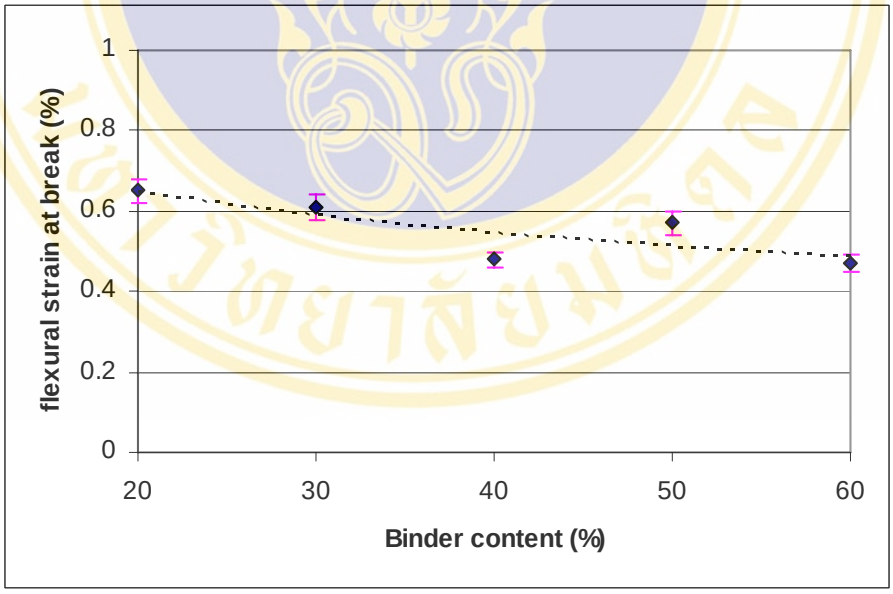

Figure 4.7 Flexural strain at break of as-fabricated samples

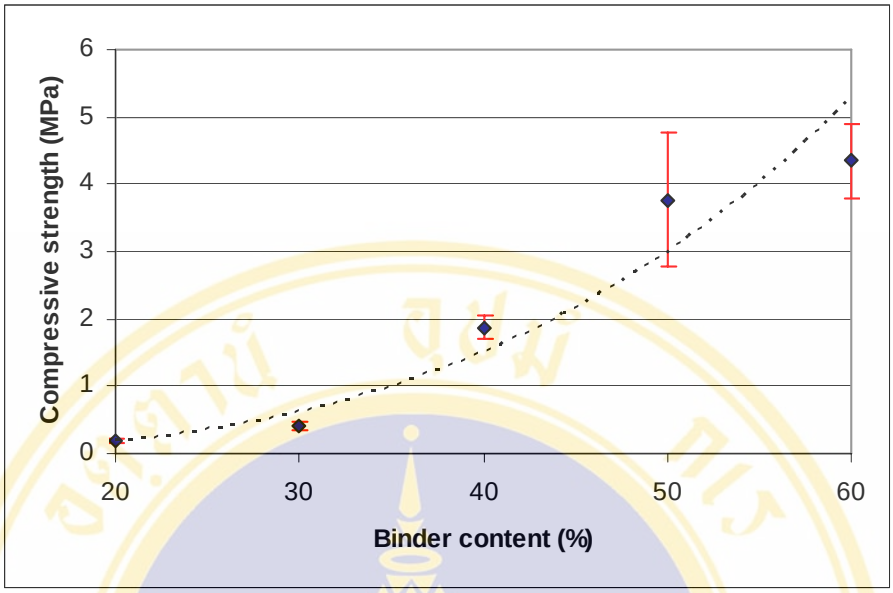

Figure 4.8 Compressive strength of as-fabricated samples

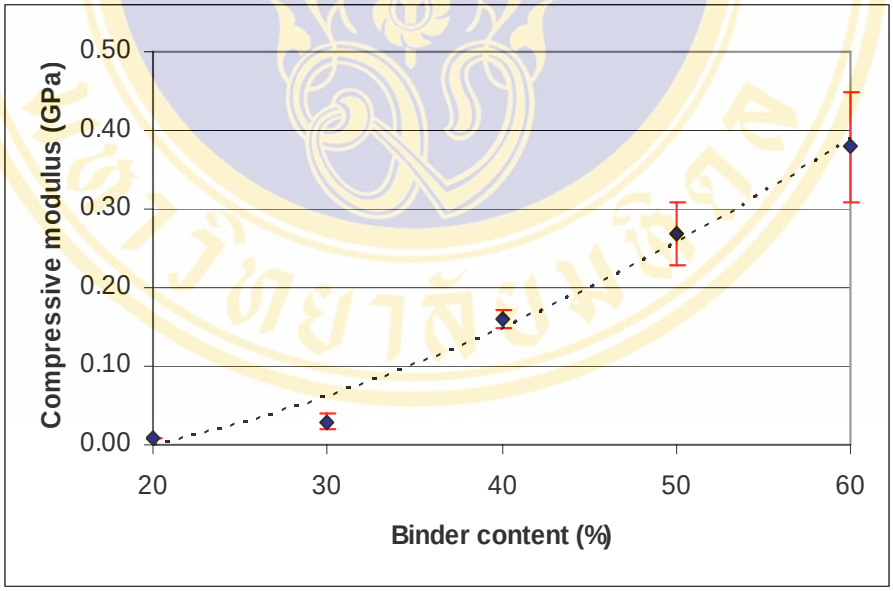

Figure 4.9 Compressive modulus of as-fabricated samples

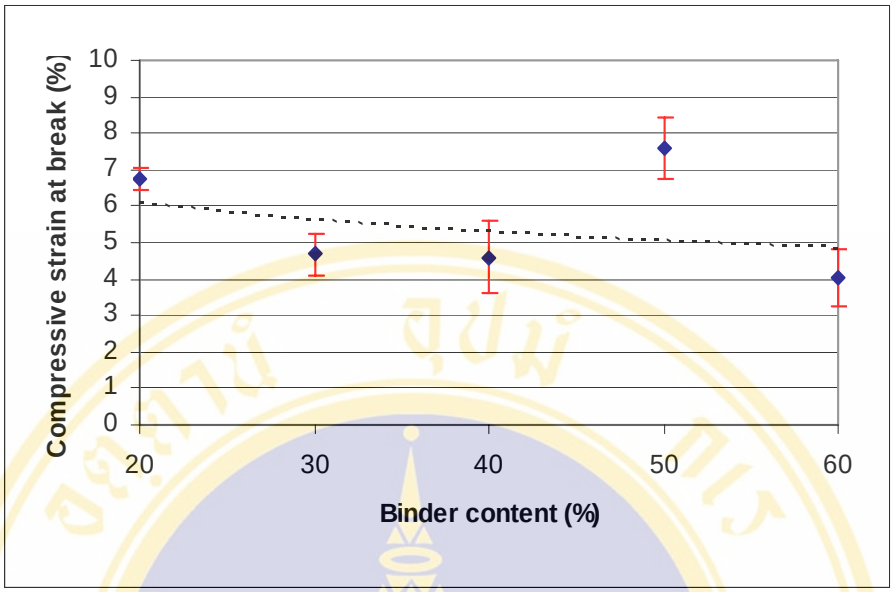

Figure 4.10 Compressive strain at break of as-fabricated samples

4.2 Infiltrated samples

4.2.1 Dimensional Change After Infiltration

The percentage of dimensional change in width, length and thickness of infiltrated samples compared to as-fabricated samples are shown in table 4.4 and Figure 4.11. At high binder content, the measured dimension in width and length was slightly lower than as-fabricated samples and the dimensional change was lower than formulations with lower binder content. However, the measured dimension in thickness was greater than as-fabricated samples in all formulations.

Table 4.4 Percentage of dimensional change after infiltration

Binder content (%)	Dimensional change (%)		
	Width	Length	Thickness
60	-1.91±0.64	-1.81±0.67	1.01±3.19
50	-1.93±2.12	-1.36±0.39	0.23±1.73
40	0.69±1.09	-0.50±0.64	3.57±0.99
30	0.80±0.95	0.27±0.26	1.78±2.64
20	1.43±1.04	0.03±0.35	5.07±1.05

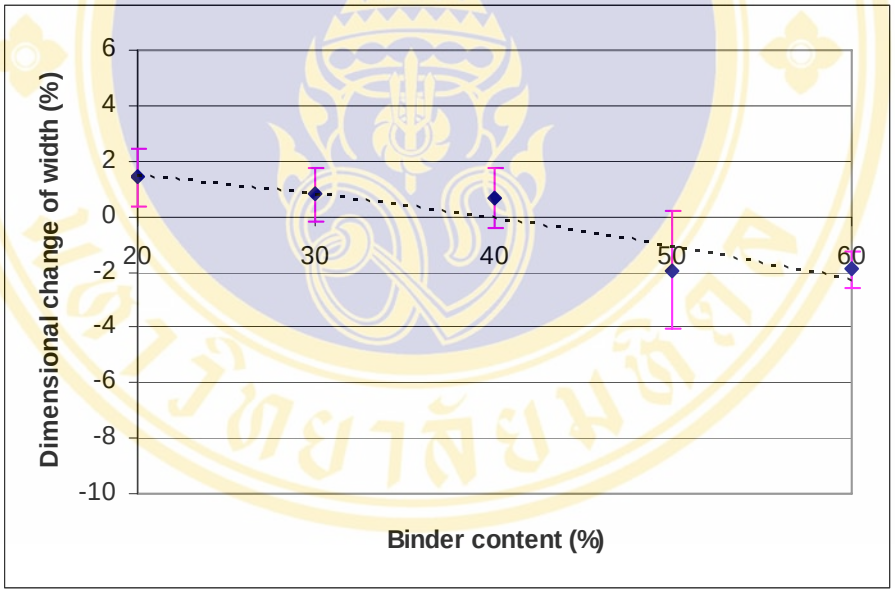

(a)

Figure 4.11 Percentage of dimensional change in (a)width, (b)length and (c)thickness after infiltration

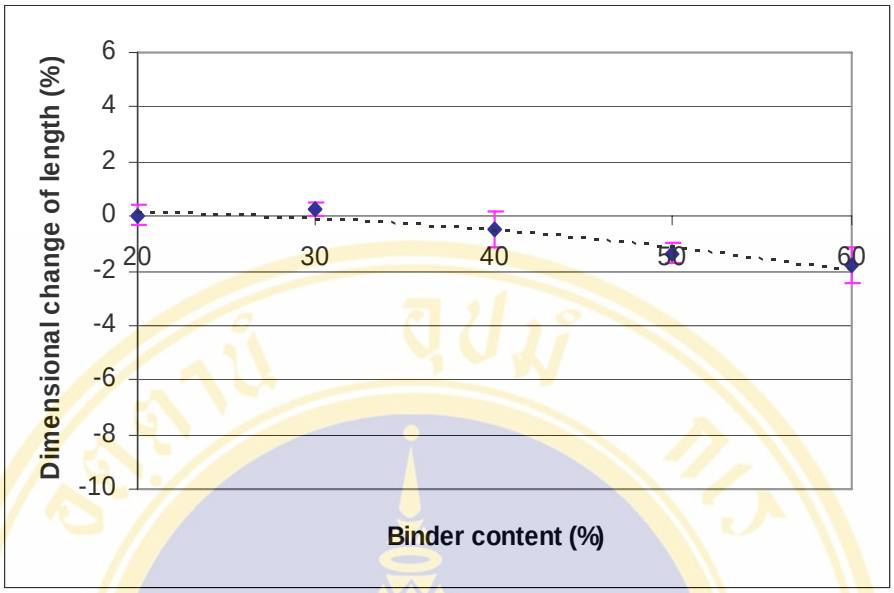

(b)

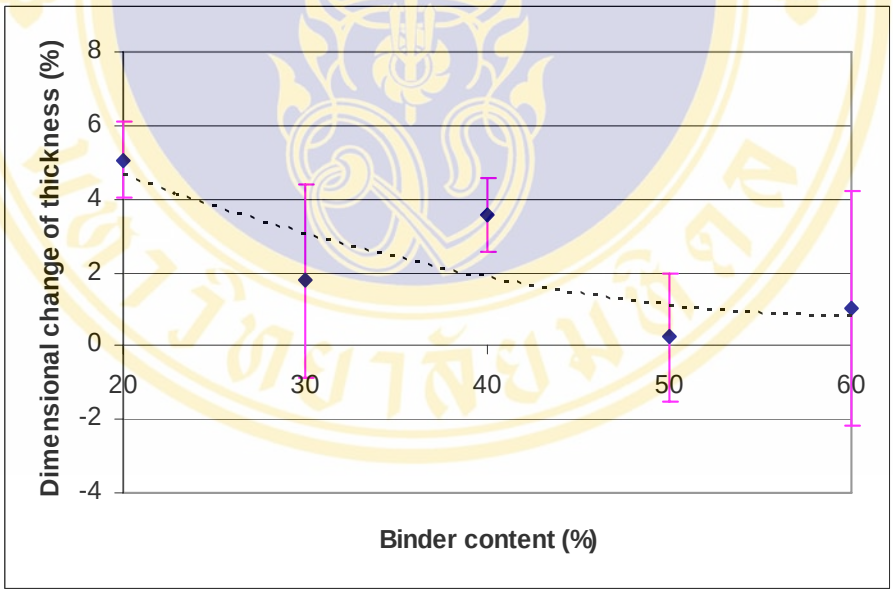

(c)

Figure 4.11 Percentage of dimensional change in (a)width, (b)length and (c)thickness after infiltration (Cont.)

4.2.2 Density and Porosity

The results indicate that increasing binder content slightly decreases bulk density but increases the percentage of porosity in the infiltrated samples (Table 4.5, Figure 4.12 and Figure 4.13).

Table 4.5 Density and porosity of infiltrated samples

Binder content (%)	Bulk density (Mg/m^3)	Porosity (%)
60	0.8778±0.04	25.70
50	0.9540±0.03	16.72
40	0.9453±0.05	11.85
30	0.9689±0.04	8.78
20	0.9491±0.02	7.98

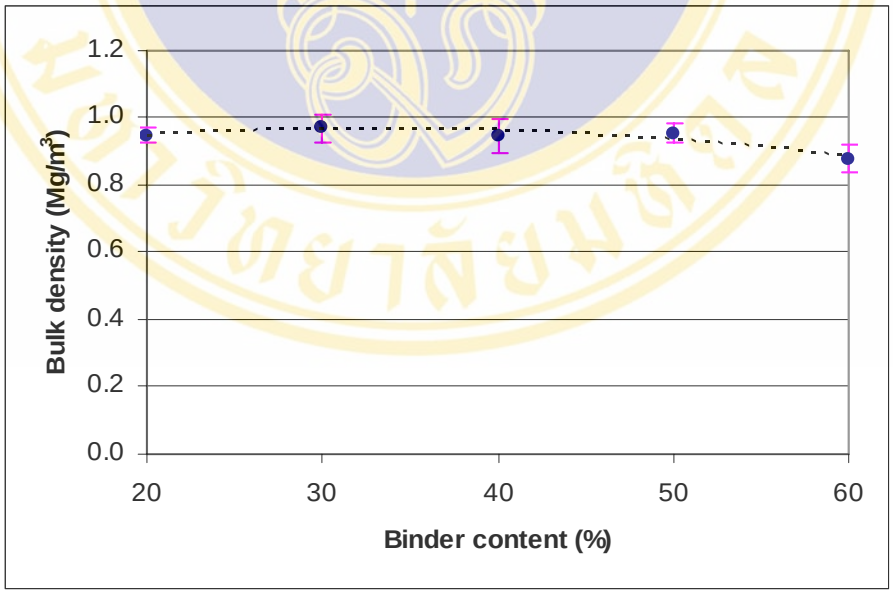

Figure 4.12 Bulk density of infiltrated samples

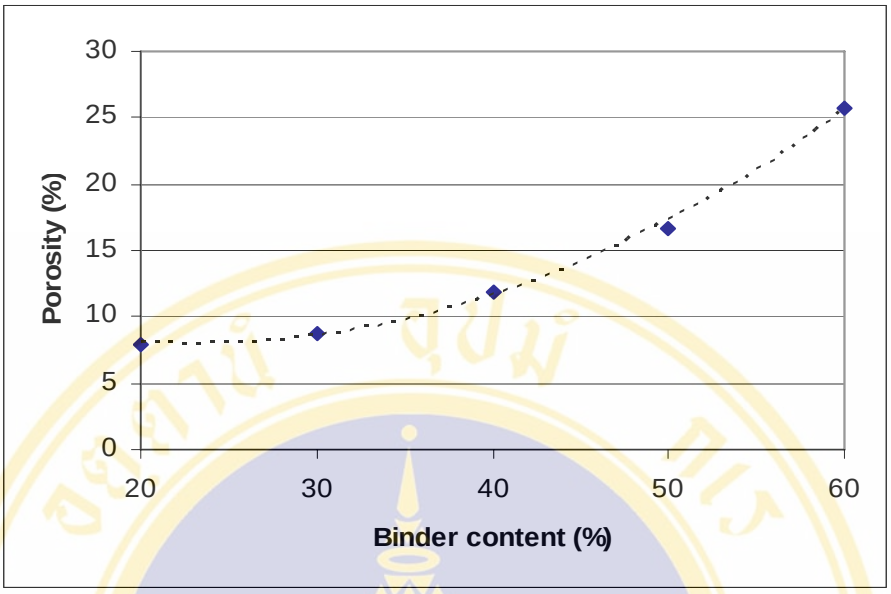

Figure 4.13 Percentage of porosity of infiltrated samples

4.2.3 Mechanical Properties

4.2.3.1 Dry condition

The mechanical properties of infiltrated samples after drying are presented in Table 4.6. The flexural strength, flexural modulus and flexural strain at break of infiltrated samples were found to increase when decreasing binder content (Figures 4.14-4.16).

The results show that compressive strength and compressive modulus increase when the amount of binder decreased similarly to flexural properties. However, compressive strain at break was not much affected by varying binder content (Figures 4.17-4.19).

Table 4.6 Mechanical properties of infiltrated samples

Binder content (%)	Strength (MPa)		Modulus (GPa)		Elongation (%)	
	Flexural	Compressive	Flexural	Compressive	Flexural	Compressive
60	6.53±0.99	26.79±2.85	1.69±0.24	0.66±0.18	0.51±0.03	17.49±2.76
50	10.88±1.79	34.05±8.04	2.04±0.13	1.09±0.14	0.65±0.14	11.87±1.48
40	17.63±2.10	41.68±6.71	2.22±0.14	1.23±0.07	0.92±0.02	8.98±0.76
30	25.20±2.18	61.68±1.57	2.46±0.30	1.31±0.08	1.13±0.10	15.70±5.53
20	31.83±2.82	72.07±8.88	2.30±0.06	1.19±0.07	1.51±0.15	24.17±12.65

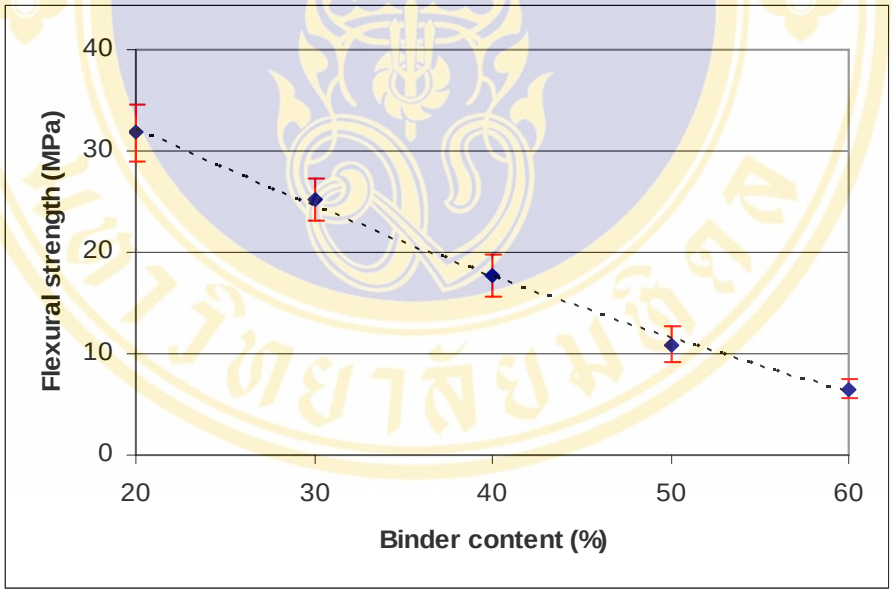

Figure 4.14 Flexural strength of infiltrated samples

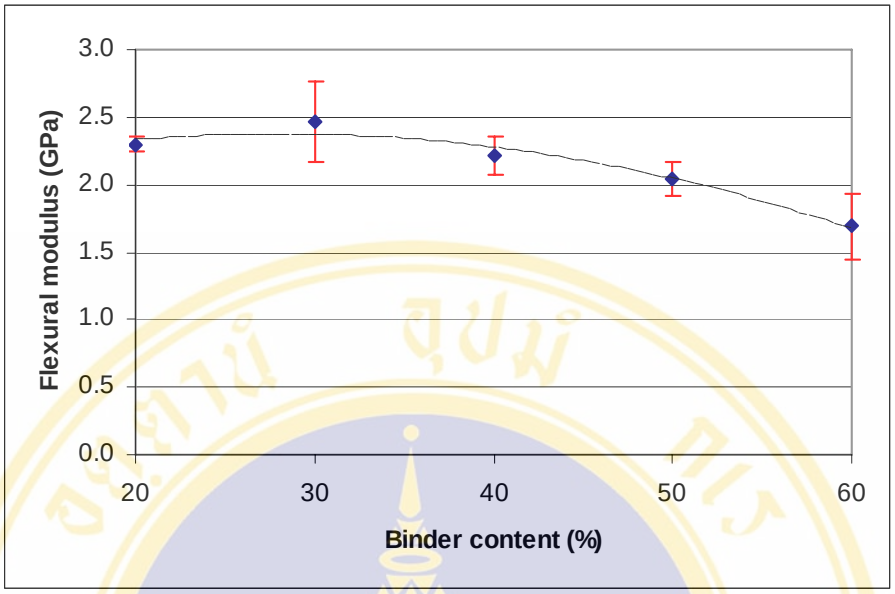

Figure 4.15 Flexural modulus of infiltrated samples

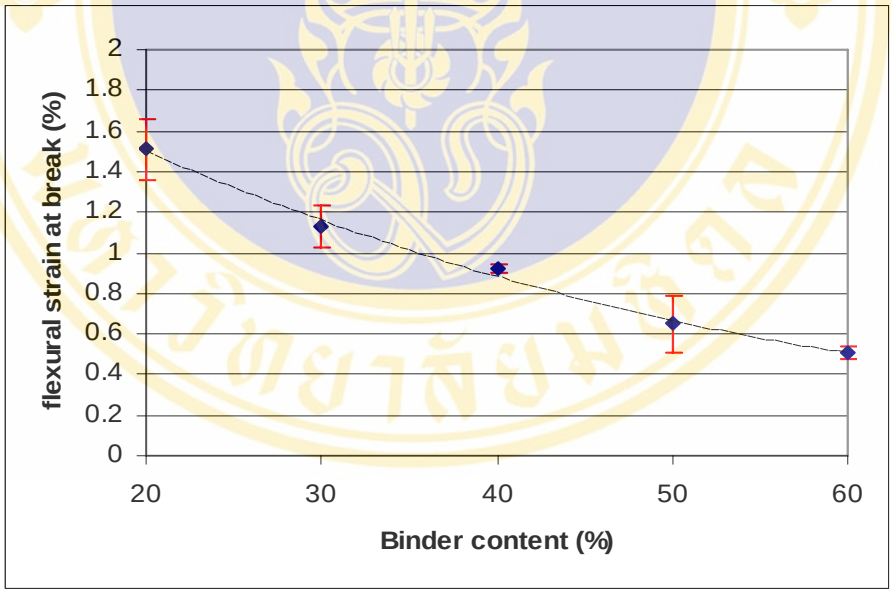

Figure 4.16 Flexural strain at break of infiltrated samples

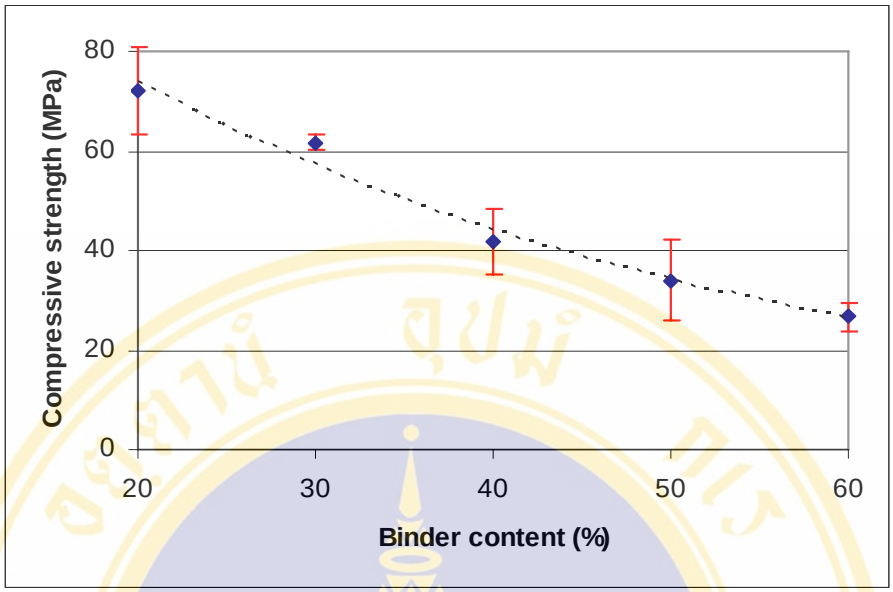

Figure 4.17 Compressive strength of infiltrated samples

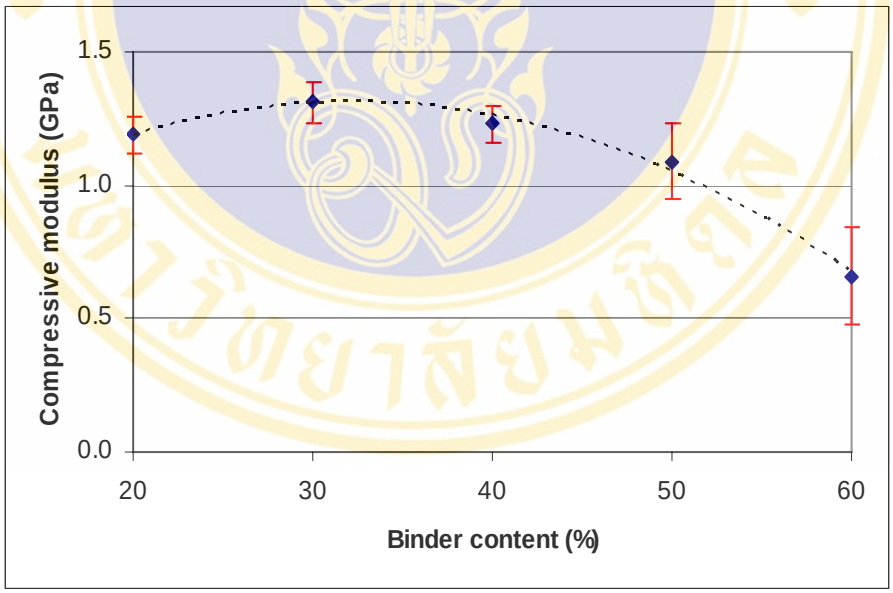

Figure 4.18 Compressive modulus of infiltrated samples

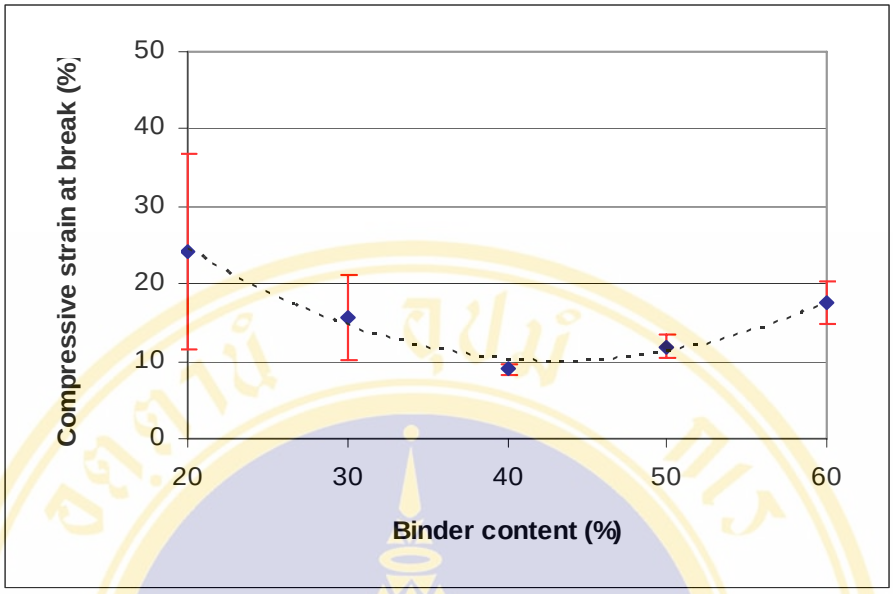

Figure 4.19 Compressive strain at break of infiltrated samples

The SEM micrographs of fractured surfaces of flexural tested specimens are shown in Figures 4.20-4.22. At low magnification (Figure 4.20) the fractured surfaces are macroscopically rough. At low binder content, the surface of the specimens becomes smoother than at higher binder formulations. This is due to the very small pore size and less porosity.

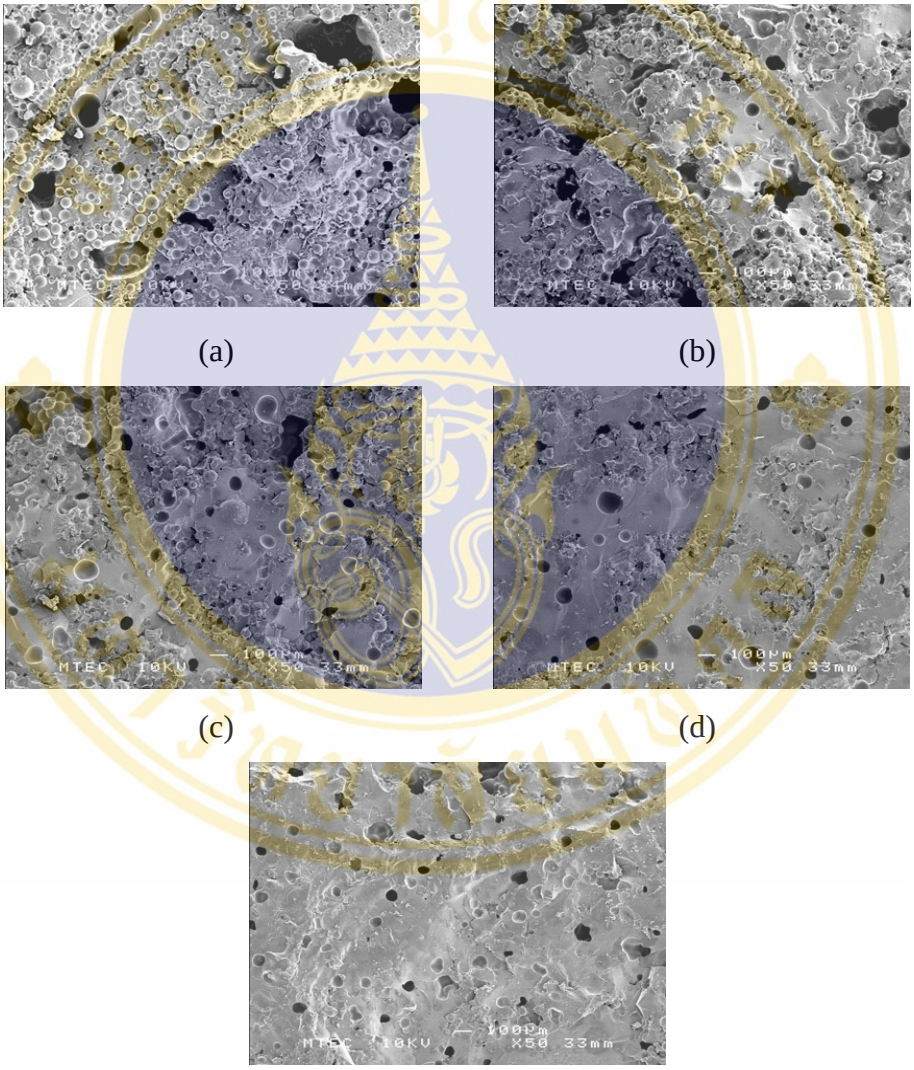

Figure 4.20 SEM micrographs of fractured surfaces of flexural tested specimens (a) 60% binder (b) 50% binder (c) 40% binder (d) 30% binder and (e) 20% binder.

At medium magnification, a smooth appearance of the particle surfaces above the fracture plane is clearly seen in high binder content formulations (a-b). A large number of particles beneath the fractured surface of the matrix had clearly separated from the matrix. It is shown that the amount of resin infiltrated in the structures is low. For lower binder content formulations (c-e), the particles are not clearly seen and appear covered by a matrix. It is shown that the amount of resin infiltrated in the structures is high.

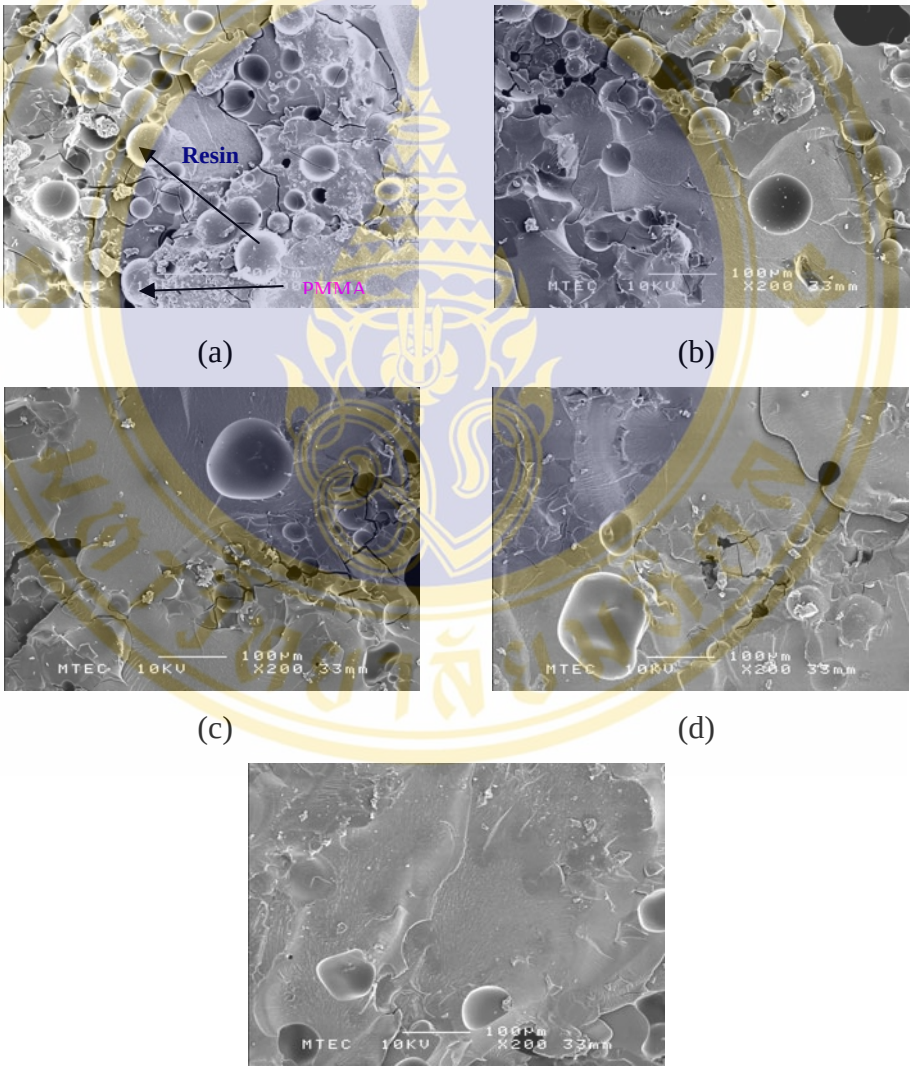

Figure 4.21 SEM micrographs of fractured surfaces of flexural tested specimens (a) 60% binder (b) 50% binder (c) 40% binder (d) 30% binder and (e) 20% binder.

The morphology at high magnification is shown in Figure 4.22. A smooth appearance of the particle surfaces is clearly seen and we can see dextrin layer connected between two PMMA particles. The interfacial debonding between infiltration resin and dextrin matrix is clearly seen at high binder formulations (Figure 4.22b) showing a poor degree of adhesion between them. When lower binder content (Figure 4.22c) we observed that PMMA particles appear covered by a matrix and the surface of PMMA particles are difficult to see. However, we can see the discontinuous phases between infiltration resin and dextrin matrix.

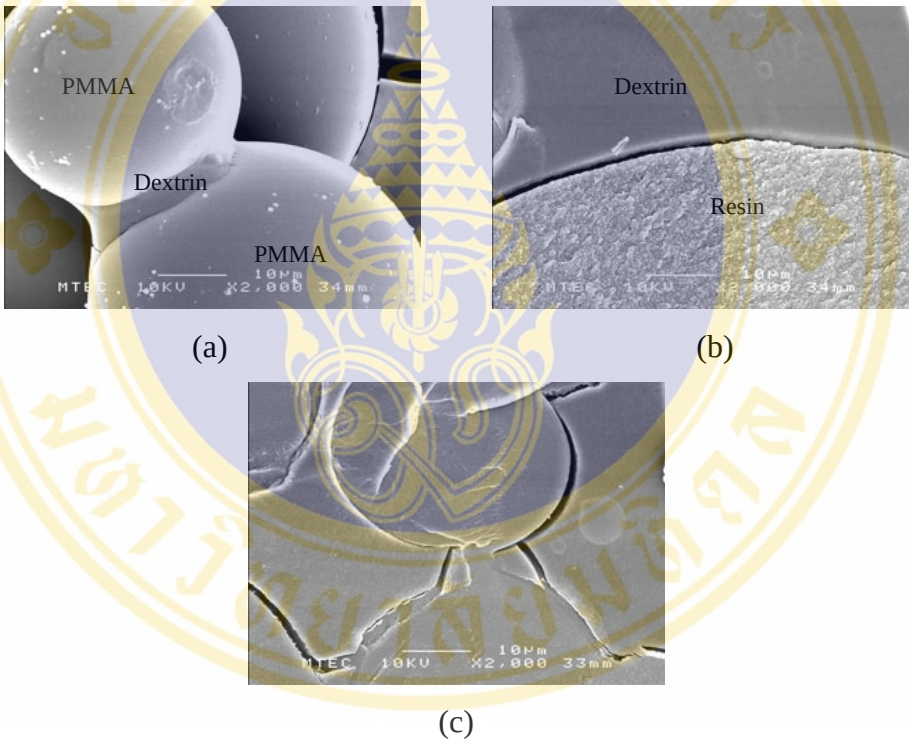

Figure 4.22 SEM micrographs of fractured surfaces of flexural tested specimens (a) 60% binder (b) 60% binder and (c) 30% binder.

4.2.3.2 Wet condition

Table 4.7 shows the average mechanical properties of infiltrated samples after soaking in water for 24 hours. The flexural strength, flexural modulus and flexural strain at break increased with decreasing binder content (Figures 4.23-4.25).

Compressive modulus and compressive strength also increased with decreasing binder content similarly to flexural properties. However, compressive strain at break did not change with varying binder content (Figures 4.26-4.28).

Table 4.7 Mechanical properties of infiltrated samples after water absorption

Binder content (%)	Strength (MPa)		Modulus (GPa)		Elongation (%)	
	Flexural	Compressive	Flexural	Compressive	Flexural	Compressive
60	2.45±0.29	4.40±1.60	0.20±0.01	0.08±0.03	1.58±0.22	17.26±3.70
50	1.34±0.24	4.37±0.77	0.14±0.01	0.10±0.01	1.91±0.21	24.86±3.93
40	6.47±0.33	15.04±1.82	0.56±0.02	0.45±0.07	1.77±0.14	25.27±2.89
30	18.34±2.49	46.03±1.61	1.01±0.06	1.01±0.06	2.32±0.30	12.01±1.20
20	25.37±1.39	71.22±8.70	1.37±0.11	1.24±0.15	2.22±0.22	24.96±4.87

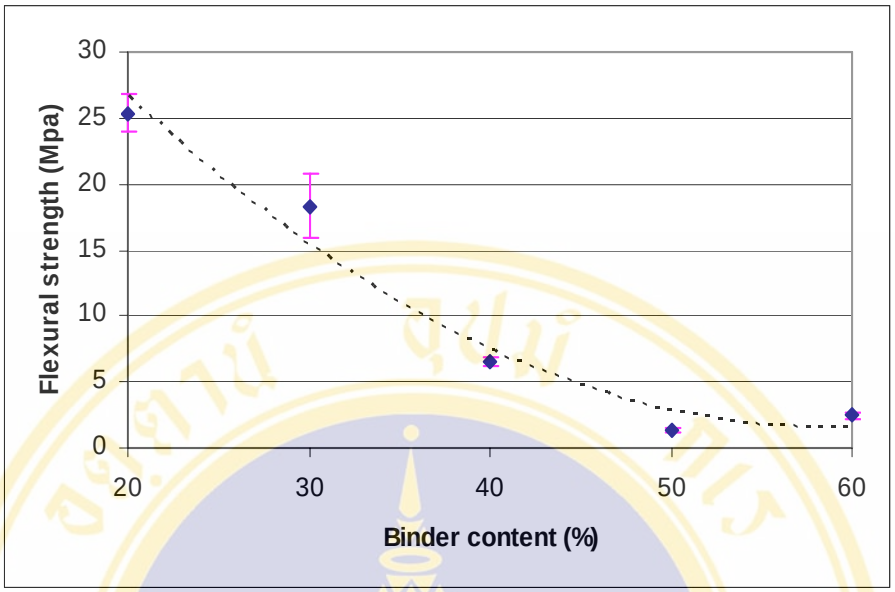

Figure 4.23 Flexural strength of infiltrated samples after water absorption

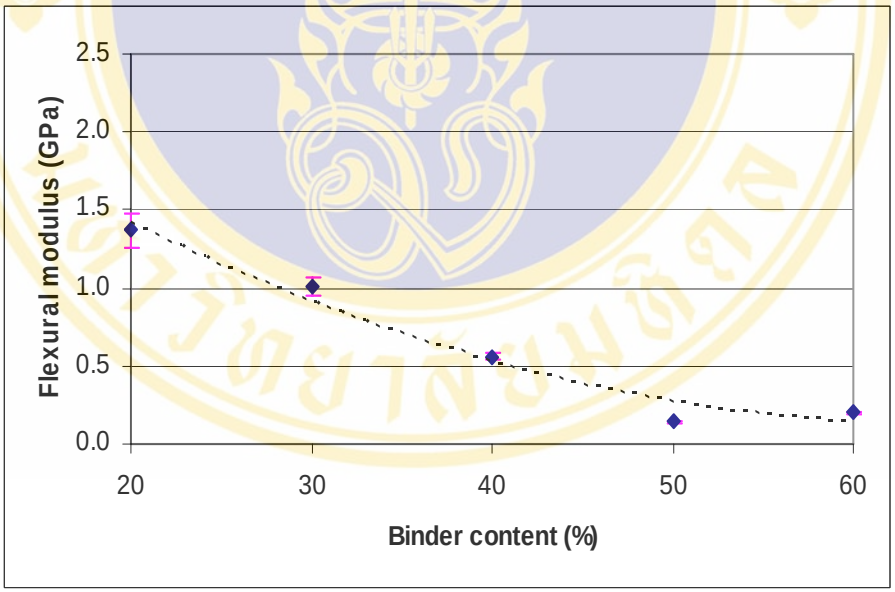

Figure 4.24 Flexural modulus of infiltrated samples after water absorption

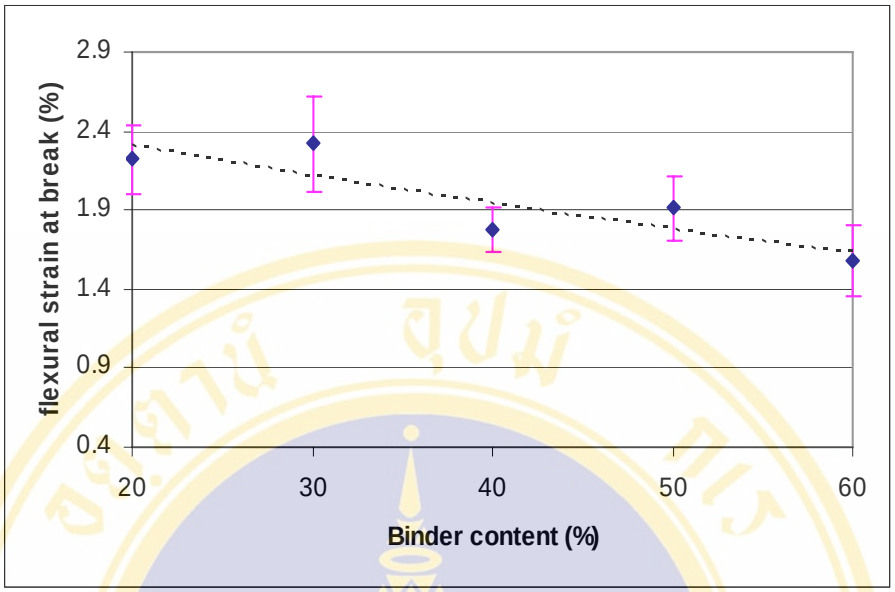

Figure 4.25 Flexural strain at break of infiltrated samples after water absorption

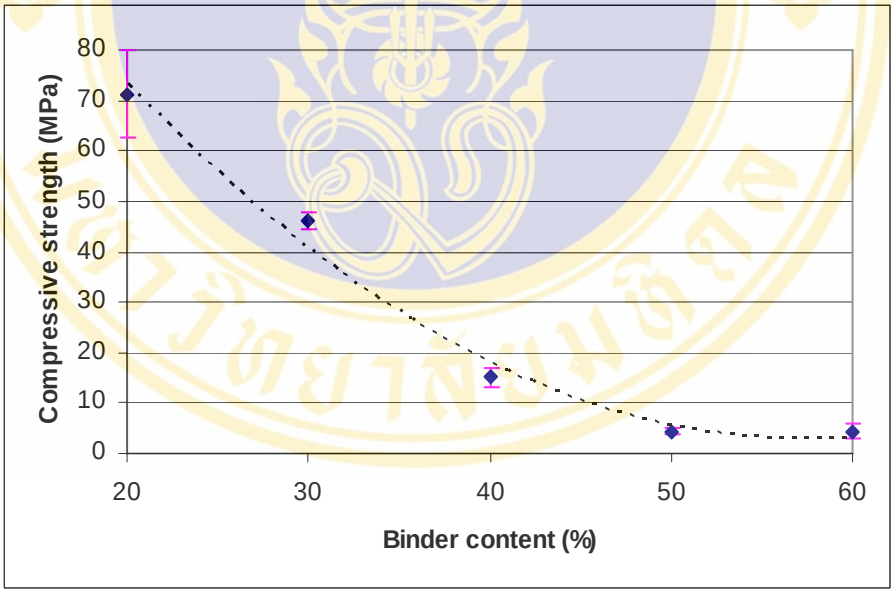

Figure 4.26 Compressive strength of infiltrated samples after water absorption

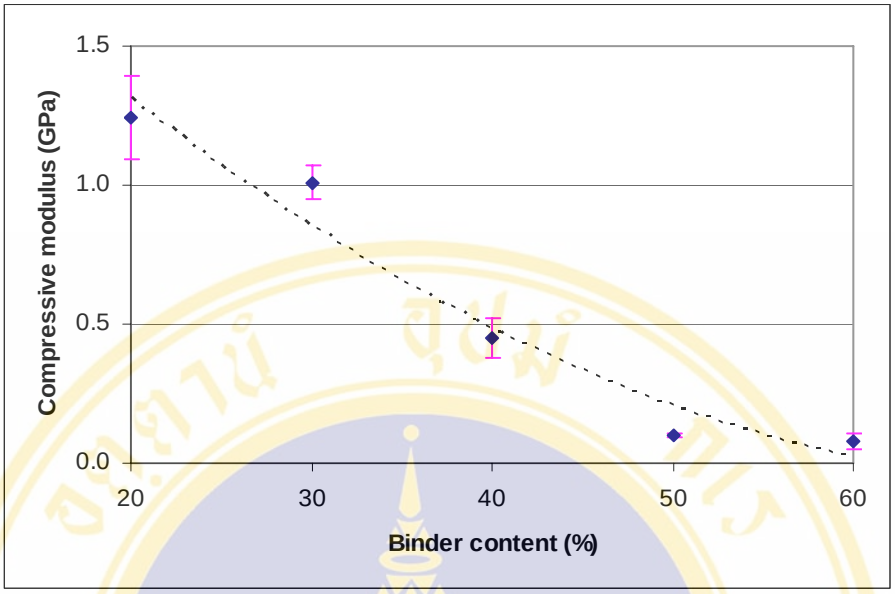

Figure 4.27 Compressive modulus of infiltrated samples after water absorption

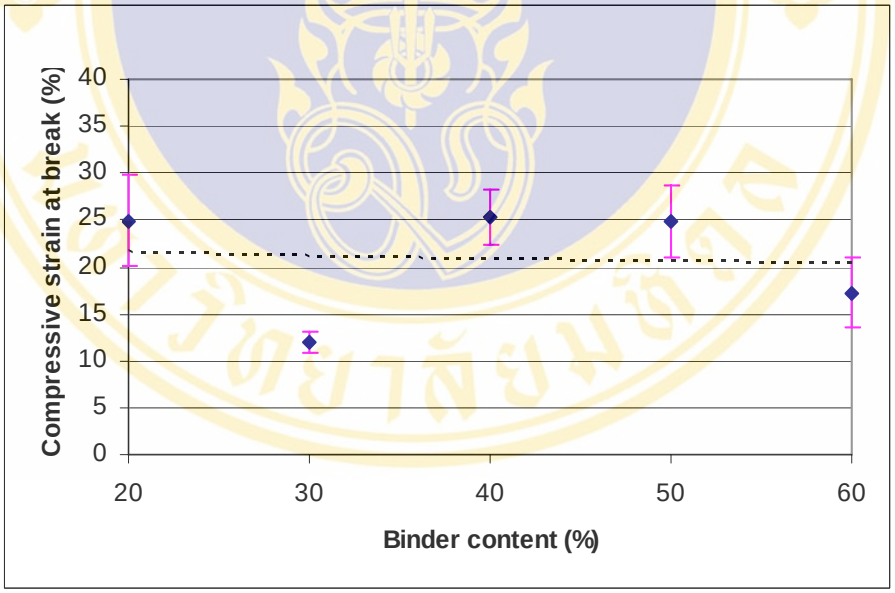

Figure 4.28 Compressive strain at break of infiltrated samples after water absorption

4.2.4 Water Absorption

The average percentage of water absorption of infiltrated samples are presented in Table 4.8 and Figure 4.29. It was found that water absorption initially increased as the amount of binder increased. However, the increase in water absorption leveled off when the binder content was greater than 40%.

Table 4.8 Water absorption of infiltrated samples

Binder content (%)	Water absorption (%)
60	3.64±0.70
50	5.70±0.55
40	3.72±0.25
30	1.83±0.09
20	0.46±0.01

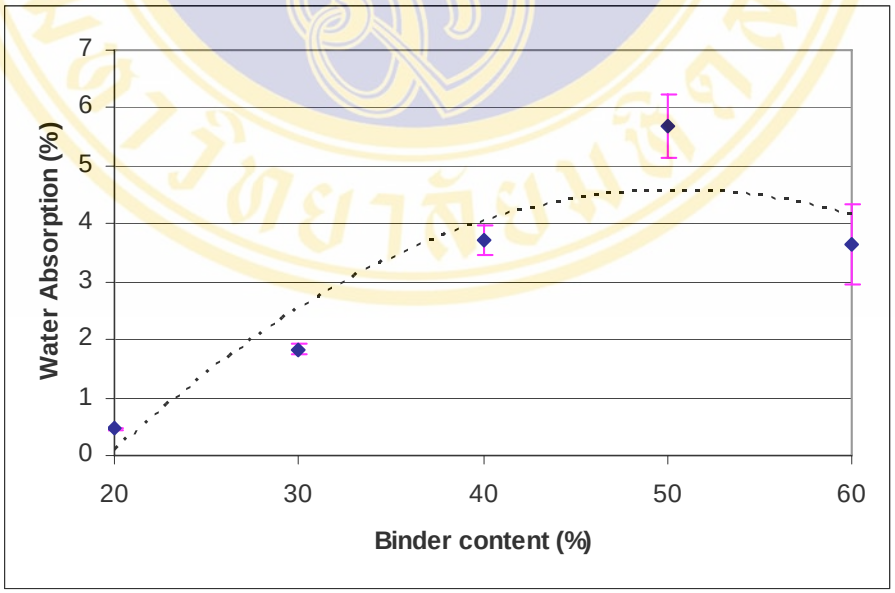

Figure 4.29 Percentage of water absorption of infiltrated samples

CHAPTER V
DISCUSSION

From the study, several points are discussed as followed.

1. Material mixture system

PMMA/Maltodextrin/PVA powder mixture was chosen as a focus material system. These materials were selected based on their biocompatibility and wetting properties with water. Many researchers [53,64] showed the potential applications of PMMA and PVA as biomaterials and maltodextrin is found in many pharmaceutical and food products [56,59]. Hence, a combination of these three materials would be a useful biomaterial. PMMA cannot be dissolved by water. Maltodextrin and PVA were chosen to act as the binding agents. Maltodextrin has high solubility which can be dissolved by the water-based binder and should bond the PMMA particles together. It can act as an adhesive of powder mixture system. PVA is a hydrophilic polymer which swells when place in water or biological fluids [60]. It has a water holding capacity and can turn to be gel after dispersion. The gel formation can trap the water in its molecule which can help preventing the shrinkage and overspreading problem.

2. Printing characteristics and green part properties

It was observed that all formulations could be fabricated by 3DP machine successfully. However, formulation 6 (0% dextrin, 10% PVA) was very fragile and was discarded from further characterization. This is thought to be due to too low amount of the component that acts as adhesive (Maltodextrin and PVA) and high amount of the matrix component (PMMA).

A comparison of dimensions between fabricated specimens of all formulations and the 3D computer image shows that the dimension control is acceptable. The maximum dimensional error of all fabricated structures was found approximately not more than 6% in all directions. As expected, the percentage of dimensional errors

in thickness was highest for all formulations. This is because the cross sections are printed in continuous strips along y-axis (cartridge travel), bands across the x-axis (gantry travel) and laminated layers along the z-axis [65]. Thus, the printing accuracy was highest along the x-axis (width) and y-axis (length) and lowest in the z-axis (thickness).

Table 5.1 Statistical Analysis of dimensional error of as-fabricated samples

Binder content (%)	Measured Dimension (mm.)			Dimensional error (%)		
	width	length	thickness	width	length	thickness
60	9.43 a	80.57 a	4.06 a	-5.70 a	0.71 a	1.40 a
50	9.52 b	80.80 b	4.14 b	-4.78 b	0.99 b	3.43 ab
40	9.53 b	80.46 a	4.08 a	-4.72 b	0.57 a	1.43 a
30	10.02 c	81.50 c	4.15 b	0.21 c	1.88 c	3.80 b
20	10.10 d	81.90 d	4.22 b	0.97 d	2.37 d	5.16 b

Means followed by a common letter are not significantly different at the 5 % level using Duncan's Multiple Range Test

From the study it can be observed that, the percentage of dimensional errors was found with both increasing and decreasing binder content. Too high or too low binder content led to the dimensional errors of the specimens. The specimens were smaller when formulations with high binder content than formulations with lower binder content. This is because the binders used in this study are water-soluble polymers. They dissolved into liquid when contacting with jetted water, which can flow through the space among PMMA particles. High amount of binder would increase the viscosity of the liquid which can be contained with lack of penetration and limit the flow distance. Higher binder content creates a large shrinkage during drying lead to the shrinkage of the part geometry of the specimens as in the formulation 1 and formulation 2. By decreasing binder content, the liquid will flow more quickly and penetration through the space among PMMA particles resulting in larger agglomerate size due to the bleeding of the liquid binder since it was less viscous and could spread outside edges of the selection. Statistical analysis using analysis of variance (ANOVA) coupled with a Duncan's Multiple Range Test (Table 5.1) showed that there was no significant difference ($p < 0.05$) in percentage of dimensional error of width between

formulation 2 and formulation 3. In the case of length, the percentage of dimensional error showed significant differences ($p < 0.05$) for all the experiment groups except formulations 1 and 3. In the case of thickness, formulations 2, 4 and 5 were greater ($p < 0.05$) than other groups. This indicates that varying amount of binder affected the percentage of dimensional error of width and length. However, the percentage of dimensional error of thickness was not much affected by varying binder content.

In the case of flexural and compressive properties, the results showed that formulation 5 which has the lowest binder content was the weakest of all the tested groups. It was observed that, increasing binder content in the formulation increased the bulk density and mechanical properties of the specimens. As the results, higher binder content increased the bulk density, strength (flexural/compressive), and modulus (flexural /compressive) of as-fabricated specimens. This is because structures fabricated by 3DP process retained their green strength at the effect of the inter-bonding by binding agent.

3. Effect of infiltration

The samples fabricated by 3DP process retained their green strength at the effect of the inter-bonding of binding agent. This is a weak bond and hence results in a relatively low green strength which is not suitable for use in medical applications. Infiltration after printing served to maintain the integrity and increase the strength of the green structures. In this research, heat-cured dental acrylic resin was selected as an infiltrant due to its nontoxicity, low viscosity, high strength and high wettability to PMMA. From the observation, the resin could fully penetrate specimens easily without the aid of external force. Analysis of variance (ANOVA) coupled with a Duncan's Multiple Range Test showed that the percentage of dimensional change in width (Table 5.2) of formulation 1 and 2 were lowest ($p < 0.05$) to other groups. There was no statistically significant difference in percentage of dimensional error of width among formulation 3-5. In the case of length, the percentage of dimensional change showed significant differences ($p < 0.05$) for all the experiment groups except formulation 4 and 5. In the percentage of dimensional change of thickness, formulation 5 were significantly superior ($p < 0.05$) to other groups.

Table 5.2 Statistical Analysis of dimensional change of infiltrated samples

Binder content (%)	Dimensional change (%)		
	width	length	thickness
60	-1.91 a	-1.81 a	1.01 ab
50	-1.93 a	-1.36 b	0.23 a
40	0.69 b	-0.50 c	3.57 bc
30	0.80 b	0.27 d	1.78 ab
20	1.43 b	0.03 d	5.07 c

Means followed by a common letter are not significantly different at the 5 % level using Duncan's Multiple Range Test.

The structural dimensions were measured before and after infiltration and there was no appreciable dimensional change. Dimensional change was found approximately not more than 6% with both increasing and decreasing binder content. Shrinkage slightly occurs at formulations with high binder content, but the increment of dimension occurs with formulations with lower binder content. This can be suggested that dimensional change was associated with moisture content change (dehydration) or the flow of the resin outside the specimens during curing process. The specimens need to be dried in the oven prior to infiltration. In addition, infiltrated specimens subjected to infiltration need to be heated in the oven in order to completely cure the heat-cured dental acrylic resin. Maltodextrin is hydrophilic and polar, it absorbs more water molecules than hydrophobic PMMA. At high binder content, high amount of maltodextrin remain in the specimens. When the specimens were dried, water molecules evaporated and can cause shrinkage. At low binder content, the amount of maltodextrin in the specimens was low but amount of resin was high. The increment of dimension can occur from the flow of resin outside the specimens before completely cure. This agreed with the observation that the shrinkage was higher when formulated with higher binder content.

The infiltrated specimens resulted in a significant improvement in its mechanical behavior under flexure and compression. The results show that the maximum flexural strength of as-fabricated structure is 1.16 MPa (60% Binder) and after infiltration is 31.83 MPa (20% Binder) thus proving the effectiveness of the infiltration method. It can be suggested that this dramatic improvement in mechanical

properties was associated with the penetration of the resin. A denser structure was linked to the high wettability of the resin for the PMMA particles so as to enable the resin to soak into the as-fabricated specimens and fill the pores.

In addition, it was observed that increasing the binder content decreased the density, flexural and compressive modulus, flexural and compressive strength of infiltrated structures. This is thought to be due to the wettability of the resin to PMMA particle is poor because the high amount of maltodextrin and low amount of PMMA in the specimens. SEM micrograph (Figure 4.21a) showed that at high binder content, the resin can not fill the whole structure and a gap between resin and PMMA particles resulted in weak structures and low strength.

SEM micrograph (Figure 5.1) came from selected region of high binder content formulations, in which high amount of maltodextrin remain on the surface of the PMMA particles so that the resin can not directly contact with PMMA particles. Therefore, the wettability of the resin to PMMA particle is poor, the boundary condition is bad. From figure 4.22b we can see that PMMA particles are poorly bonded with the matrix phase (maltodextrin) and are distributed in the dextrin matrix discontinuously. This agreed with the observation that the density and mechanical properties of the structures were reduced.

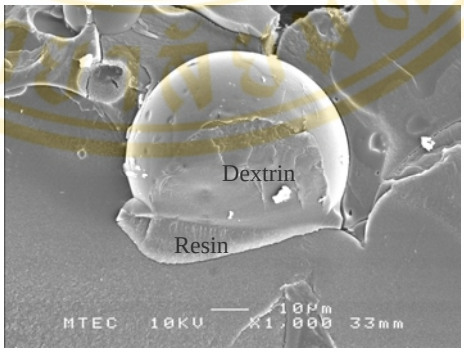

Figure 5.1 SEM micrograph of flexural fracture of infiltrated PMMA samples with 50% binder

4. Effect of water absorption

Mechanical properties of infiltrated specimens conditioned in water for 24 hours (Figure 5.2-5.5) were evaluated. It was found that the results followed the same trend as those obtained in dry specimens. A significant decrease in flexural strength, compressive strength, flexural modulus and compressive modulus were noticed for all specimens except in formulation 5 (Table 4.6 and 4.7). Formulation 5 with a flexural strength of 25.4 MPa and compressive strength of 71.2 MPa were significantly superior to other formulations and did not reveal any significant decrease in flexural and compressive strength compare to dry specimens. Flexural strength and compressive strength from formulation 1 and 2 were not statistical different from each other. After soaking in water, a 20–80% reduction in flexural strength, and 1-87% reduction in compressive strength for infiltrated specimens were noted. It can be suggested that the decrement in strength and modulus was associated with the porosity of the structure and polar of binding materials. Since maltodextrin is hydrophilic and polar, maltodextrin absorbs more water molecules than hydrophobic PMMA. Moreover, maltodextrin has high solubility which can be dissolved in water. So, decreasing the percentage of maltodextrin in the powder mixture also decreases absorption of water molecules (as in formulation 5). At low binder content, the structures were dense, high wettability of the resin to PMMA and low amount of maltodextrin, thus enable the structures to restrict the penetration of water molecules.

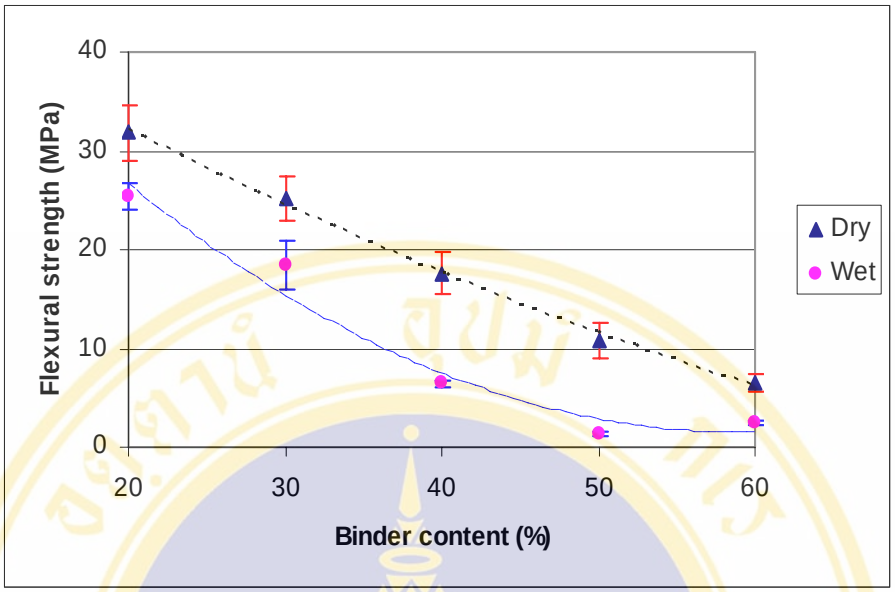

Figure 5.2 Flexural strength of dry and wet specimens

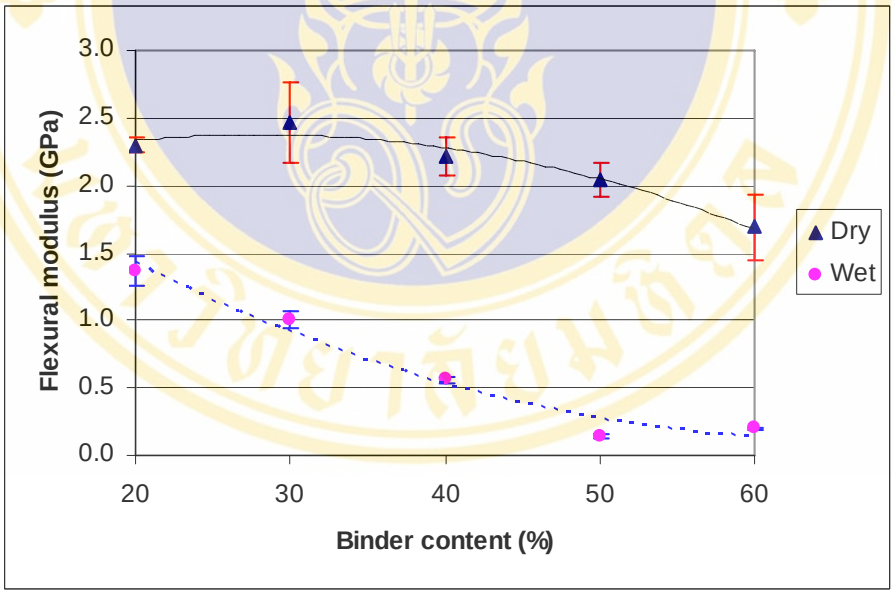

Figure 5.3 Flexural modulus of dry and wet specimens

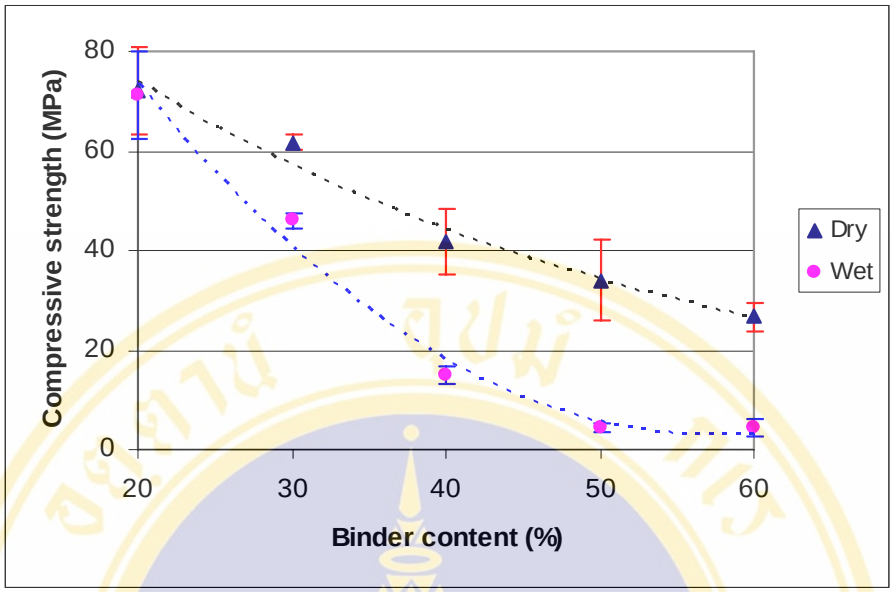

Figure 5.4 Compressive strength of dry and wet specimens

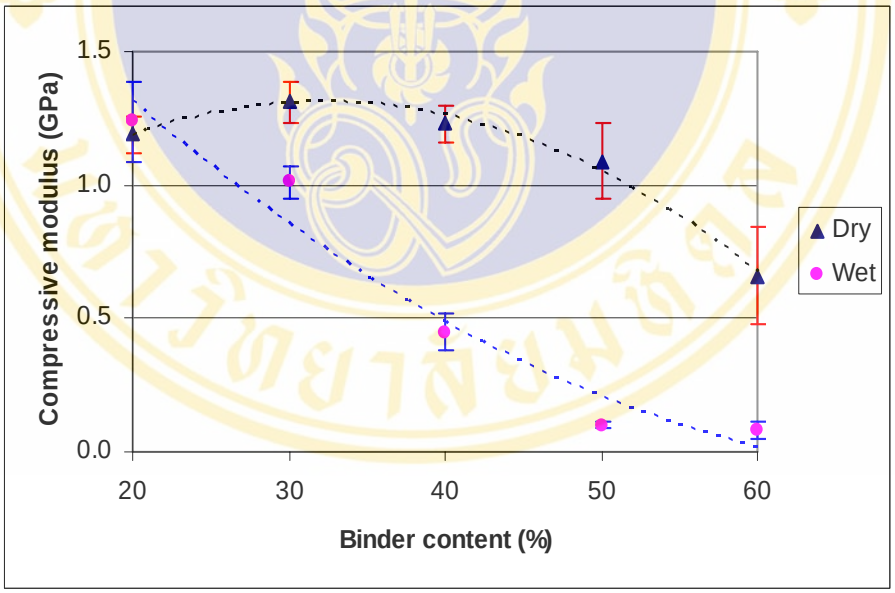

Figure 5.5 Compressive modulus of dry and wet specimens

5. Comparison infiltrated samples with commercially heat-cured and self cured PMMA specimens

The infiltrated specimens were compared with indirect fabricated heat-cured polymethyl methacrylate and commercially self-cured polymethyl methacrylate specimens in terms of flexural modulus and flexural strength (Figures 5.6-5.7). In the case of compressive properties, the infiltrated specimens were compared only with indirect fabricated heat-cured polymethyl methacrylate specimens (Figures 5.8-5.9).

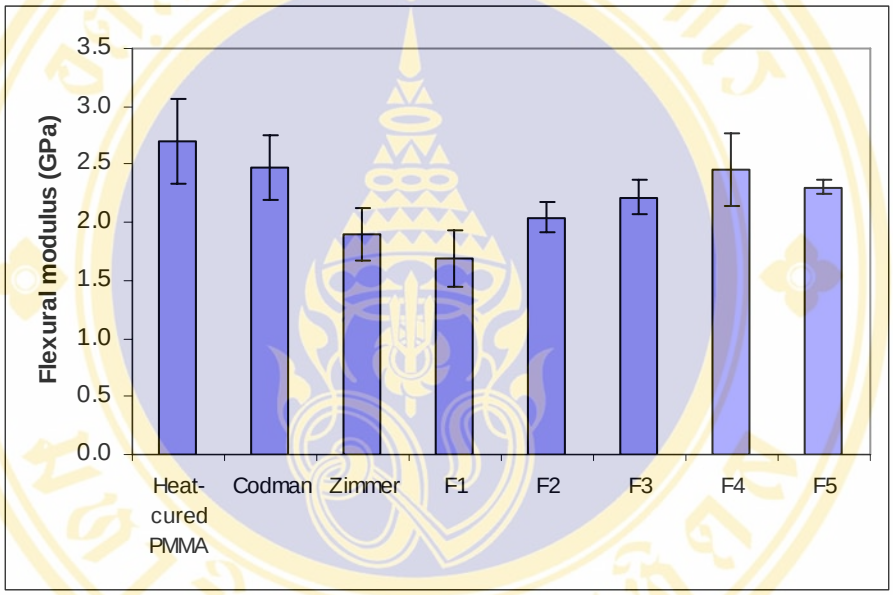

Figure 5.6 Flexural modulus of specimens

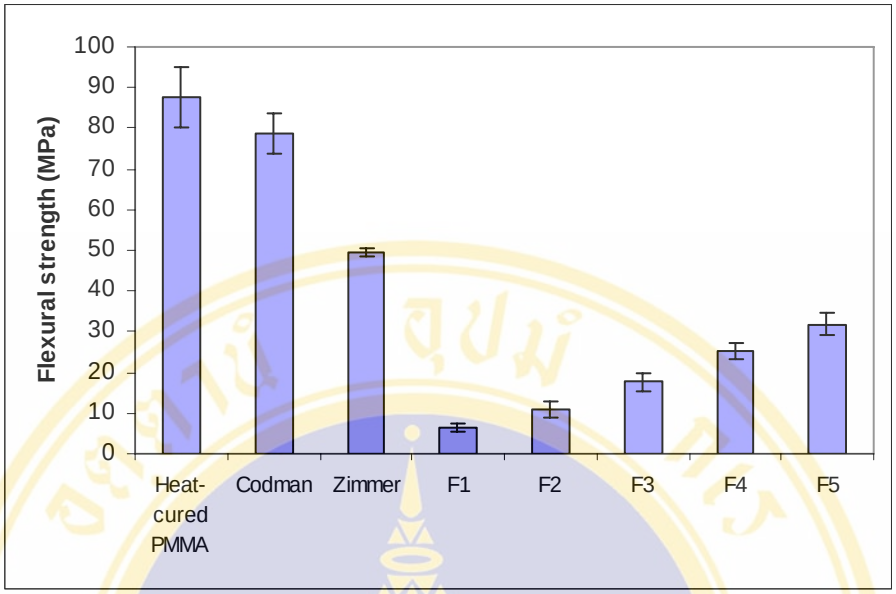

Figure 5.7 Flexural strength of specimens

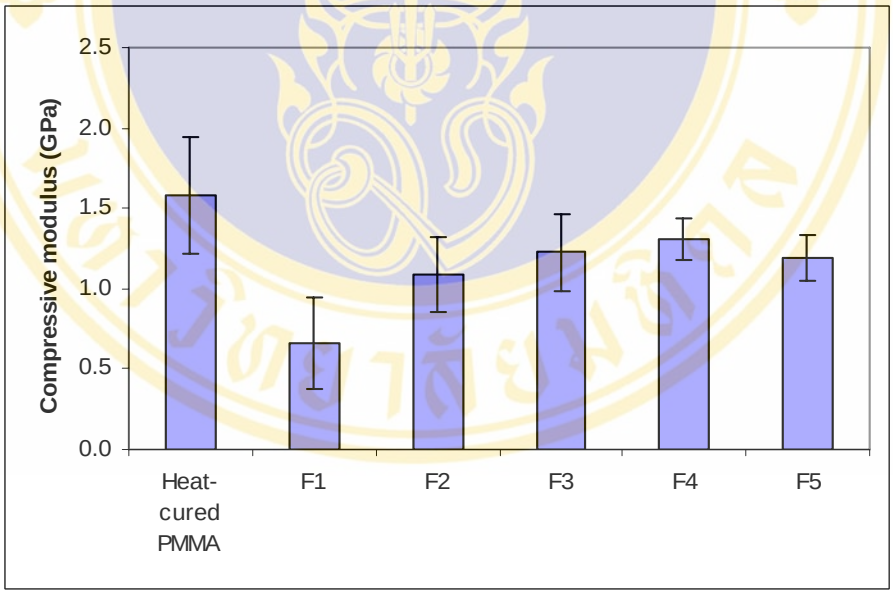

Figure 5.8 Compressive modulus of specimens

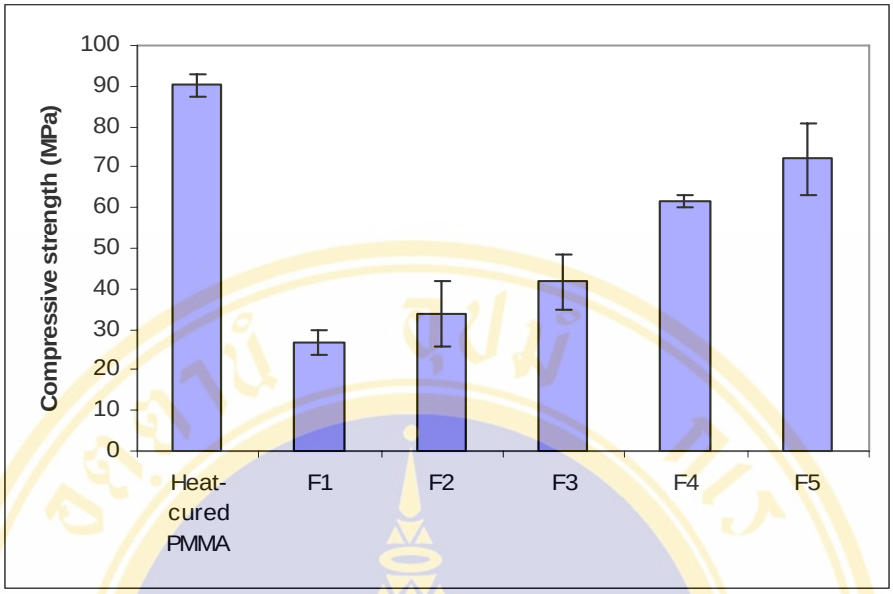

Figure 5.9 Compressive strength of specimens

In comparison to reference samples (indirect fabricated heat-cured PMMA, Codman® and Zimmer®) the results showed that the flexural modulus of tested samples were close to the values of Zimmer®, Codman® and indirect fabricated heat-cured PMMA. In the case of flexural strength, the infiltrated specimens were approximately 60% of the values of Zimmer®, 40% of the values of Codman® and 35% of the values of indirect fabricated heat-cured PMMA.

In comparison to heat-cured PMMA in the case of compressive properties, the results showed that the compressive modulus of infiltrated samples were close to the values of heat-cured PMMA except in formulation 1 (F1). In the case of compressive strength, the infiltrated specimens were approximately 80% of the values of indirect fabricated heat-cured PMMA.

6. Implant fabrication of optimized formulation

We have found that, the optimum formulation for the best mechanical results was determined to be 80% PMMA, 10% maltodextrin and 10% PVA (Formulation 5) , however the formulation for the best dimensional results consisted of 70% PMMA, 20% maltodextrin and 10% PVA (Formulation 4). Therefore, the suitable amount of binder should be chosen to optimize between strength and physical properties. The optimum formulation should be formulation 5 because this formulation

exhibits highest mechanical strength. Dimensional error in the formulation can be incorporated in the design as well as in the 3D model in order to compensate this dimensional or geometrical change.

The selected formulation (formulation 5) was chosen for trial to directly fabricate real complex bony structure. It was found that the implant for maxilla replacement could be printed successfully without problem. Figures 5.10-5.12 show the PMMA implant, along with the skull model fabricated by traditional plaster-based materials. It can be seen that the PMMA implant can fit nicely to the defected part on the model. This proves the possibility of direct fabrication of PMMA by raw materials in this study.

Figure 5.10 PMMA implant fabricated by three dimensional printing

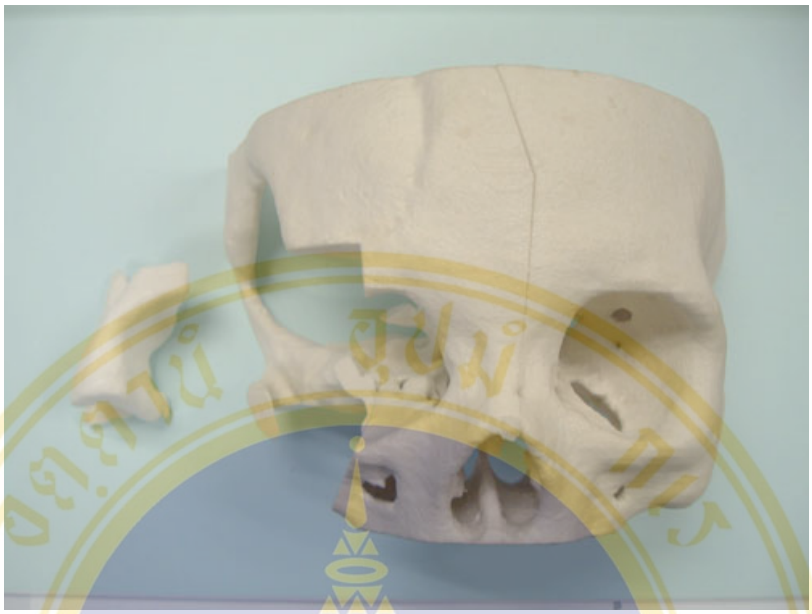

Figure 5.11 3DP model of patient's skull defect and final PMMA implant

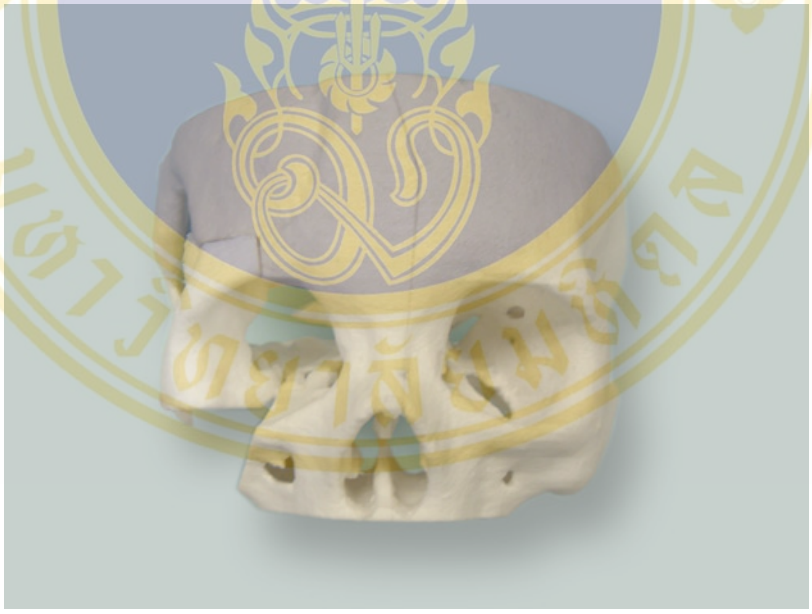

Figure 5.12 Precise fitting of PMMA implant and patient's skull model

CHAPTER VI
CONCLUSION

From the results presented in this thesis it was concluded that:

1. Polymethyl methacrylate structures were successfully direct fabricated by three-dimensional printing technique using 100% saturation and 0.175 mm layer thickness.
2. The optimum formulation was 80% PMMA, 10% maltodextrin and 10% Polyvinyl alcohol.
3. Using low binder content for as-fabricated part fabrication was more favorable if the parts are designed to be post-processed by heat-cured resin infiltration. However, the binder content should not be too low and sufficient for specimens handling prior to infiltration.
4. Increasing binder content in the formulation decreased the porosity of the as-fabricated specimens but increased the bulk density, flexural and compressive properties of the specimens. However, increasing or decreasing binder content of the specimens both led to the dimensional errors of the specimens.
5. Infiltration by heat-cured acrylic resin enhanced modulus, strength of structures to be closed to conventional indirect fabricated PMMA resin. Increasing binder content in the formulation increased the porosity of the infiltrated specimens but decreased bulk density and mechanical properties which is in contrast to the behavior of as-fabricated specimens.
6. In comparison to commercial PMMA previously used for indirect fabrication, it was observed that the modulus of infiltrated samples could be tailored to be closed to the commercial PMMA. In the case of strength, compressive strength of infiltrated samples was slightly lower than the commercial PMMA whereas the flexural strength was approximately one third. It is expected that the materials and

process developed in this study could be used as an alternative for the fabrication of PMMA parts from indirect fabrication process.

7. The ability to fabricate a complex-shaped by this technique would aid in customization of pre-surgical implants.

Future Work

This thesis builds a foundation for further research in fabricating sufficient strong and dimensional accurate complex-shaped PMMA parts by three-dimensional printing technology. For further development, research directions should be investigated:

1. Improve the mechanical properties of PMMA structure

In comparison to commercial PMMA previously used for indirect fabrication, the modulus and strength of infiltrated samples were still lower than the commercial PMMA. From the study, the infiltrated specimens (optimum formulation) have 8 % porosity. This is indicated that there are some pores and air bubbles remain in the specimens. Since the cracks in the specimen are initiated at pores which act as stress risers and fatigue failure in test specimens occurs almost through such pores. The routes which should be investigated to improve the mechanical properties of the specimens are the search for filler materials for packing the pores to reduce the porosity and bubbles in the specimens; and the improvement of infiltration method such as by drawing a vacuum on or pressurizing the part while it is in an infiltrant bath for forcing the infiltrant into the pores of the part.

2. Determination of the optimum printing parameters

In this study, the printing parameters have been set to 100 % saturation and 0.175 mm layer thickness. This appears to be a safe value that avoids the problem of the layer slippage [66]. More experiments, however, are needed to determine how the percentage of saturation and thickness should be set.

REFERENCES

1.Vaandrager JM, Zonneveld FW, Mathijssen IMJ, Hovius SER. First Generation 3D Model of a Noma Patient - A Case Report: Planning and Surgery. Phidias Newsletter. December 1998; 1: 6-7.

2. Wouters K. Colour Rapid Prototyping – An Extra Dimension for Visualising the Human Anatomy. Phidias Newsletter. June 2001; 6:4–5.

3. Berry E, Brown JM, Connell M, Craven CM, Efford ND, Radjenovic A, Smith MA. Preliminary experience with medical applications of rapid prototyping by selective laser sintering. Medical Engineering and Physics. 1997;19:90–96.

4. Haex TH, Bijvoet HWC, Dallenga AHG. The Use of Stereolithographic Models in Patients with Large Cranial Defects. Phidias Newsletter. December 1998; 1: 4-12.

5. Popat AH. Rapid prototyping and medical modeling. Phildias Newsletter. December 1998; 1:10-12.

6. Josip B. Rapid prototyping in reconstruction of large calvarial defects. Phidias Newsletter. December 1999; 3:3.

7. Jacobs P. Stereolithography and Other Rapid Prototyping and Manufacturing Technologies. Dearborn, MI, American Association of Engineers Press, 1996.

8. Weiss LE. Chapter 2 : Processes Overview. Rapid Prototyping in Europe and Japan (Final Report). 1997;1: 5-7.

9. Galanter P. Rapid Prototyping Additive Technologies That Will Reshape Design & Manufacturing.Connect: Information Technology at NYU, Spring 2004;3.

10. Burghilde M, Wieneke T, Hans WG. Rapid Prototyping Technology – New potentials for offshore and abyssal engineering. Wieneke, University of Applied Sciences, Dept. VIII , Paper No. 2003.

11. Mcmains S. Rapid Prototyping of Solid Three-Dimensional Parts. Master's Project, Department of Electrical Engineering and Computer Science, University of California, Berkeley.1995: 6.

12. Ryall C and Wimpenny D., editors. [monograph on the Internet] ;c2003. Rapid Prototyping for Rapid Castings, The Rapid Prototyping & Tooling Centre, Warwick Manufacturing Group, University of Warwick [cited 2005 Jul 12]. Available from: http://www.jharper.demon.co.uk/rptc01.htm

13. Dolenc A. An Overview of Rapid Prototyping Technologies in Manufacturing. Institute of Industrial Automation, Helsinki University of Technology. July1995:6-11.

14. Grimm T. Stereolithography, Selective Laser Sintering and PolyJet™: Evaluating and Applying the Right Technology. Accelerated Technologies, Inc., 2002.

15. Marais J. Complex Shaped Mold Manufacturing by means of Laminated Object Manufacturing, Center for Composite Materials Technical Report CCM. 2003-08.

16. Winder J, Bibb R. Medical Rapid Prototyping Technologies: State of the Art and Current Limitations for Application in Oral and Maxillofacial Surgery. Americal Association of Oral and Maxillofacial Surgeons. 2005: 1108-1010.

17. Mcmains S. Rapid Prototyping of Solid Three-Dimensional Parts. Master's Project, Department of Electrical Engineering and Computer Science, University of California, Berkeley.1995: 11-13.

18. Gould LA, editor. Quick Look at Rapid Prototyping, Automotive Design & Production [monograph on the Internet]. Gardner Publications, Inc.; c2000 [cited 2005 Aug 10]. Available from: http://www.autofieldguide.com/articles/090101.html

19. Friedrich BP, Clinton LA, Richard FA. Rapid Prototyping in Europe and Japan. Analytical Chapters. March 1997; 1:14-16.

20. Lukkassen D, Meidell A. Advanced Materials and Structures and their Fabrication Processes, 4. th edition, Narvik University College, HiN. August 2005: 231-232.

21. Ali KK, Sengupta S. Prototyping and Rapid Prototyping Concepts. Industrial and Manufacturing Systems Engineering Department, The University of Michigan-Dearborn, Dearborn. MI 48128-1491.

22. Robert SS, editor. Rapid Prototype: No longer Just for Design Engineer [monograph on the Internet]. Wikipedia the free encyclopedia [cited 2005 Aug 9].
Available from:
http://www.jobshoptechnology.com/features/0305/prototyping.shtml

23. Castle Island Co. [homepage on the Internet]. Castle Island's Worldwide Guide to Rapid Prototyping ;c2005. The Most Important Commercial Rapid Prototyping Technologies at a Glance [cited 2005 Jul 12].
Available from: http://home.att.net/~castleisland/rp_int1.htm

24. Ashley S. Rapid Prototyping for Artificial Body Parts. Mechanical Engineering. May 1993:50-53.

25. Potamianos P, Amis AA, Forester AJ, McGurk M, Bircher M. Rapid prototyping for orthopaedic surgery. Journal of Engineering in Medicine. 1998; 212: 383-393.

26. Yay Y, Arvier JF, Barker TM. Technical note: Maxillofacial biomodeling - preliminary result, British Journal of Radiology.1995; 68: 519-523.

27. Nishiyama T, Nakajima T, Yoshimura Y, Nakanishi Y. Utilising solid models for preoperative shaping of HAP-TCP ceramic bone substitute: application for craniomaxillofacial surgery, European Journal of Plastic Surgery. 1994; 17: 173- 177.

28. Kermer C. Preoperative stereolithographic model planning in craniomaxillofacial surgery, University Clinic for Maxillofacial Surgery, University of Vienna, Austria. Phidias Newsletter. June 1999; 2: 1-3.

29. Preliminary Experience with Selective Laser Sintering Models of the Human Temporal Bone, Americal Journal of Neuroradiology.1994;15: 473-477.

30. Cheng AC, Wee AG. Reconstruction of cranial bone defects using alloplastic implants produced from a stereolithographically - generated cranial model. Annals Academy of Medicine Singapore. Sep 1999; 28(5):692-696.

31. Dallolio V, Orsi M, De Micheli E, Monolo L, editors. CAD Case studies, Custom cranioplasty with PMMA using rapid prototyping and 3D CAD [monograph on the Internet]. Neurosurgical Unit, Lecco Hospital, Lecco, Italy and Ing.; c2005. [cited 2005 Jul 29].

Available from: http://www.materialise.com/mimics/case15_ENG.html

32. ScienceDaily. The Plasti-Bone: Office Of Naval Research Looks At A Ceramic Polymer Innovation In Medicine [monograph on the Internet].; June c2003. [cited 2006 April 30].
Available from:
http://www.sciencedaily.com/releases/2003/06/030616090308.htm
33. Constans A. Machining the Body: Rapid prototyping techniques promise better design and fabrication of tissue-engineering scaffolds. The Scientist. May 2005; 19: (9)4-7.
34. Seitz H, Rieder W, Irsen S, Leukers B, Tille C. Three-Dimensional Printing of Porous Ceramic Scaffolds for Bone Tissue Engineering. Wiley InterScience, January 2005; 782-788.
35. Hollister SJ, Lin CY, Saito E, Lin CY, Schek RD, Taboas JM, Williams JM, Partee B, Flanagan CL, Diggs A, Wilke EN, Van Lenthe GH, Muller R, Wirtz T, Das S, Feinberg SE, Krebsbach PH. Engineering craniofacial scaffolds. Orthodontics and Craniofacial Research.2005; 8:162-173.
36. Sharke P. Rapid Transit to Manufacturing, Mechanical Engineering. March 2001:1-6.
37. Ashley S. Rapid Prototyping is Coming of Age. Mechanical Engineering. July 1995; 117(7) 62-68.
38. Mironov V, Boland T, Trusk T, Forgacs G, Markwald R. Organ Printing: Computer-aided Jet-based 3D Tissue Engineering. Trends in Biotechnology 2003; 21: 4.
39. Yan Y, Zhang R, Lin F. Research and Application on Bio-Manufacturing, International Conference on Advanced Research in Virtual and Rapid Prototyping. 1-4 October 2003: 23-29.
40. ผศ. ทพ. วิจิตร ธรานนท์, ดร.จินตมัย สุวรรณประทีป, บทที่3 ขั้นตอนการสร้างหุ่นจำลองทางการแพทย์ด้วยการสร้างต้นแบบรวดเร็ว, *เทคโนโลยีการสร้างต้นแบบรวดเร็วทางการแพทย์และทันตกรรม*, พิมพ์ครั้งที่ 1, ศูนย์เทคโนโลยีโลหะและวัสดุแห่งชาติ (เอ็มเทค), กรุงเทพมหานคร: กุมภาพันธ์ ; 2549.
41. Jawaharlal Nehru Cancer hospital and Research centre. Diagnostic Facilities:CT Scan. [homepage on the Internet].[cited 2006 July 15].

Available from: http://jnch.nic.in/infra.htm#diag

42. Puttre M. Replacing Parts On Nature's Machines. Mechanical Engineering. May 1993:58- 61.
43. Swalens B, Kruth JP. Medical Application of Rapid Prototyping Techniques. 4th International conference on Rapid Prototyping. 14-15th June,1993, pp 107-120.
44. Computer-Aided Medical Technology Laboratory, MTEC, Thailand. (2005) Rapid Prototyping in Medicine. Power Point Tutorial. Thailand.
45. Davis JR, Davis & Associates. Polymeric materials. Handbook of Materials for Medical Devices. Second ed ,2004:151-159.
46. Francis B, Quinn JR, Matthew WR. Chin and Malar Implants. Grand Rounds Presentation, UTMB, Dept. of Otolaryngology. March 31, 2004.
47. McGrath JE, Wilkes GL, Ward T. ACS Polymer Short Course Notes. 2001.
48. Kine BB, Novak RW. Acrylic and Methacrylic Ester Polymers. in Encyclopedia of Polymer Science and Engineering, Wiley: New York, 1985; 262.
49. Davis JR, Davis & Associates. Polymeric materials. Handbook of Materials for Medical Devices. Second ed ,2004;217-218.
50. Tangram Technology. Polymer Data File:Polymethyl Methacrylate -PMMA (Acrylic) [homepage on the Internet]. Tangram Technology.,Ltd ; c2000 [cited 2005 Aug 28].

    Available from: http://www.tangram.co.uk/TI-Polymer-PMMA.html
51. Buddy DR, Allan SH. An Introduction to Materials in Medicine. Biomaterials Science.1996; 2.
52. Taha F, Lengele B, Boscherini D, Testelin S. Modeling and design. Phidias Newsletter.2001; 6.
53. Vangool AV. Preformed Polymethylmethacrylate Cranioplasties. Journal of Maxillo - facial Surgery.1985;13:2-8.
54. Emma J, Hollick BA, editors. Intraocular lens implantation [monograph on the Internet]. City University London: Association of Optometrists, ; c2001 [cited 2005 September 30].

Available from:
http://www.optometry.co.uk/files/c61abd5f535b595ad793073458afed7c_hollick20011102.pdf

55. Toyoshima T. Biomaterial Research in Japan. Embassy of Finland. 2001; 9.

56. Carvalho JM, Gama FM. Hydrogels of Enzymatically Modified Dextrin. Centro de Engenharia Biológica, Universidade do Minho. Campus de Gualtar, 4710-057 Braga, Portugal.p.1.

57. Erickson A. Corn Starch. Corn Refiners Association, Inc. 10th Edition: 2004; 14-15.

58. Shree Additives. Dextrin [homepage on the Internet]. Wall Street - II, Opp, Orient Club, Ellisbridge, Ahmedabad: Shree Additives (Pharma and Foods) Ltd; c2000 [cited 2005 September 30].
Available from: http://www.shreeadditives.com/htmlsite/6f.htm

59. Benton R. Determination of Maltodextrin in Pharmaceutical and Food Products. Food and Beverage Metrohm-Peak, Inc. The Application Notebook. June 2004; 40.

60. Hassan C, Peppas N. Structure and Applications of Poly(vinyl alcohol) Hydrogels Produced by Conventional Crosslinking or by Freezing /Thawing Methods. Advances in Polymer Science. Springer. 2000; 153: 37-62.

61. Laurence M and Sharp DWA. A new dictionary of chemistry, 4th ed. Wiley, New York. 1968.

62. Finch CA. Poly(vinyl alcohol): Properties and Applications. Wiley, New York.

63. Tanigami T,Yano K, Yamaura K, Masuzawa S. Polymer. 1995; 36: 2941.

64. Oka M, Naguchi T, Kumar P, Ikeuchi K, Yamamuno T, Hyon SH, Ikada Y. Clinical Materials.1990; 6: 361.

65. Z Corporation. Z 400 System User's Manual. Part number 09500, Revision C, 1997-2002: 1-8.

66. Tesavibul P. Development of Novel Biomaterials for 3DP based on Natural Polymers. Master Thesis, Biomedical Engineering Programme, Faculty of Graduate Studies Mahidol University, Bangkok; Thailand, 2004.

BIOGRAPHY

NAME Miss Pantida Patirupanusara

DATE OF BIRTH 22 April 1974

PLACE OF BIRTH Chainat, Thailand

INSTITUTIONS ATTENED Mahidol University ,1993-1996
Bachelor of Science
(Biotechnology)
National Institute of Development
Administration ,1998-1999
Graduated Diploma Program
(Information System
Development)
Mahidol University ,2002-2006
Master of Engineering
(Biomedical Engineering)

HOME ADDRESS 259/318 Soi Phibun Wet, Sukhumvit 71
Rd., Phrakhanong, Wattana
Thailand 10110
E-mail : pantida@hotmail.com